UNIVERSITÀ DEGLI STUDI DI MILANO

Dipartimento di Scienze della Salute

Corso di Dottorato in

Medicina Clinica e Sperimentale

XXIX ciclo

High-resolution spatiotemporal analysis of Somatostatin Receptor Type 2 (SSTR2) - Filamin A (FLNA) interaction by single-molecule imaging

Tesi di Dottorato di: Donatella Treppiedi

Matr. n°: R10592

Tutor: Prof.ssa Giovanna Mantovani

Anno Accademico 2015-2016

INDEX

SUMMARY

Somatostatin receptor type 2 (SSTR2) is the main pharmacological target to treat different neuroendocrine tumors, including pituitary GH-secreting adenomas. Nevertheless, a subset of acromegalic patients, i.e. patients with a GH-secreting tumor, is not fully controlled by the medical therapy, and the molecular mechanisms underlying the pharmacological resistance to somatostatin analogues (SSAs) are not completely understood. Recently, the cytoskeletal protein Filamin A (FLNA) has been implicated in the regulation of tumor responsiveness by modulating SSTR2 expression and signaling.

The aims of the present study were to explore the *in vivo* dynamics of FLNA-SSTR2 interactions at the plasma membrane and the involvement of FLNA in the modulation of SSTR2 distribution and mobility. To this purpose, single-molecule imaging experiments were performed at the Institute of Pharmacology and Toxicology, University of Würzburg (Würzburg, Germany), at Dr. Davide Calebiro's lab. We also wanted to evaluate the impact of FLNA-SSTR2 binding on ligand-induced SSTR2 clusters organization and internalization.

First, the motion of freely diffusing SSTR2 particles was observed to slow down upon CHO cells exposure to 100nM BIM23120. The trajectories of SSTR2 particles were used to calculate their diffusion coefficient through mean square displacement (MSD) analysis. A significant increase in the SSTR2 fraction with diffusion coefficient values $\leq 0.05 \mu m^{2*} s^{-1}$ with was detected in stimulated cells compared to unstimulated cells (28,1% *vs* 14,4%, expressed as fraction of total particles, respectively, $P < 0.05$). The presence of the FLNA truncated mutant, that selectively prevents SSTR2-FLNA binding (FLNA 19-20), did not influence the SSTR2 agonist effect on receptor mobility. Such data were further confirmed in melanoma cell lines. Then, we described the nature of the interactions between SSTR2 particles and FLNA fibers as extremely dynamic and transient under resting condition, whereas they resulted long-lasting and more stable after BIM23120

treatment. Interestingly, when both FLNA and SSTR2 were expressed at single molecule level, FLNA-SSTR2 complexes formation was seen to occur preferentially along actin filaments, in stimulated cells only. Furthermore, when overexpressed and stimulated, SSTR2 was observed to undergo clusters formation, and FLNA-SSTR2 binding was required to preserve SSTR2 clusters alignment on actin structures as well as their colocalization with the clathrin coated pits marker AP-2. In addition, quantitative analysis of the agonist-triggered SSTR2 internalization demonstrated a significant reduction of the internalization rate in the presence of FLNA 19-20 compared to negative control (FLNA 17-18), at all the tested time points (eg. 45,3% ± 1,4% internalization *vs* 71,4% ± 3,1% in FLNA 19-20 *vs* FLNA 17-18 transfected cells after 30min stimulation with 100nM BIM23120, respectively, $P < 0,001$), accordingly with biotinylation results.

In conclusion, the behavior of FLNA-SSTR2 interactions were characterized for the first time by means of a high spatio-temporal resolution strategy. Altogether these results support a crucial role of FLNA in the recruitment of ligand-activated receptors and in their anchorage to the cortical actin cytoskeleton with important consequences on the overall SSTR2 internalization process.

1. INTRODUCTION

1.1 SOMATOSTATIN AND ITS RECEPTOR FAMILY

1.1.1 Somatostatin structure

Somatostatin (SS), or somatotropin release-inhibiting factor, is a small cyclic peptide widely expressed throughout the central nervous system (CNS) and in several peripheral tissues such as the peripheral nervous system, pancreas, gut, thyroid, retina and others. In humans, there exists only one gene encoding for SS, located on chromosome 3q28 . The first mRNA product is a 116 amino acids precursor termed prepro-SS; this larger polypeptide is then processed to pro-SS of 92 amino acids, and finally to SS-28 and SS-14, the two biologically active forms consisting of 14 and 28 amino acids, respectively (Brazeau et al., 1973) (Fig. 1). SS-28 comprises SS-14 and a NH2-terminal extension (Fig. 2) (Shen et al., 1982) and encountered for only the 20-30% of the SS expressed in the brain.

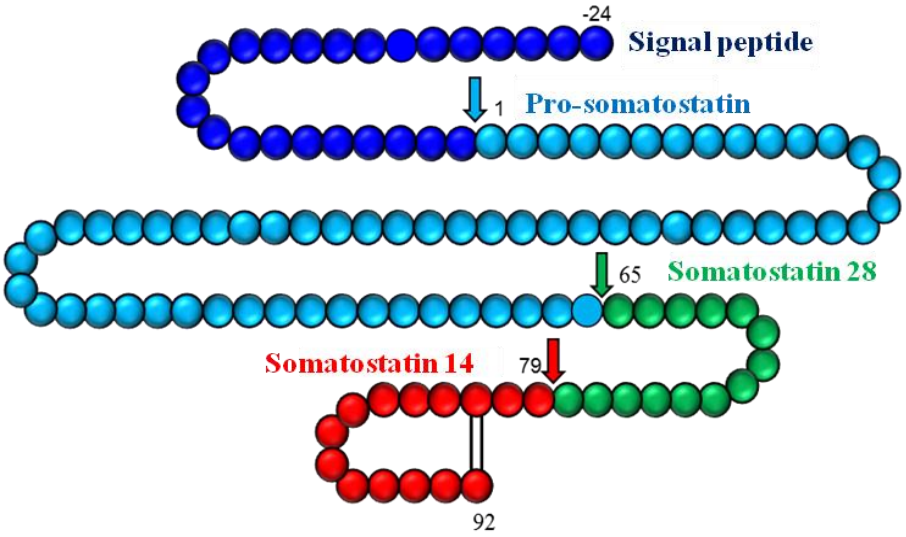

Figure 1. Illustrative picture of the SS precursor. Pro-SS (92 amino acids), SS-28 (28 amino acids) and SS-14 (14 amino acids) originate from the grater polypeptide prepro-SS.

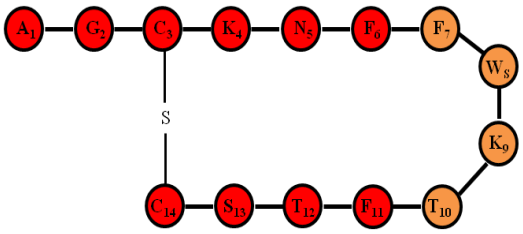

Figure 2. Amino acid sequence of the active form SS-14. Amino acid residues, Phe[7], Trp[8], Lys[9] e Thr[10], crucial for SS biological functions, are depicted in orange.

1.1.2 Biological actions of SS

SS plays a variety of biological functions accordingly to its location. In the CNS, SS acts as a neurotransmitter with both stimulatory and inhibitory effects on cognitive functions and locomotor activity. In fact, alterations of the somatostatinergic transmission at this level, have been related to different neurologic disorders, such as Alzheimer disease (Grouselle et al., 1998), HIV-encephalopathy (Fox et al., 1997), Huntington's disease (Beal et al., 1988), Parkinson's disease (Strittmatter et al., 1996), and temporal lobe epilepsy (Strowbridge et al., 1992).

SS has a broad range of actions, almost exclusively inhibitory, on endocrine and exocrine gland secretion. SS is a crucial inhibitor of GH (Brazeau et al., 1973; Bertherat et al., 1995), TSH (Siler et al., 1974), ACTH (Richardson & Schonbrunn, 1981; Batista et al., 2006), and PRL release (Vale et al., 1974) from the anterior pituitary. Although the main effect of SS is to prevent hormonal exocytosis, *in vitro* and *in vivo* experiments have shown suppression of GH and ACTH transcription through SSTR2 action, as well (Castillo et al., 2011; Ben-Shlomo et al., 2013).

At the peripheral nervous system level, SS controls the gastrointestinal tract activity by blocking the release of several hormones: colecystochinin, gastric inhibitory peptide, gastrin, motilin, neurotensin and secretin (Sheratori el al., 1991). Moreover, SS regulates bowel motility and gastric emptying, smooth muscles contraction, and nutrient absorption from the intestine. SS also suppresses the exocrine secretory action of pancreas, inhibiting glucagon, insulin and pancreatic polypeptide release (Stark & Mentlein, 2002; Ludvigsen et al., 2007). In the kidney, SS blocks

renin secretion (Gomez-Pan et al., 1976) and ADH-mediated water absorption (Reid & Rose, 1977), and in the adrenal gland prevents angiotensin II-stimulated aldosterone release and decreases catecholamines levels induced by acetylcholine.

SS plays other inhibitory effects on growth factors (IGF-1, EGF, PDGF) and cytokine release from immune cells (IL6, IFN-β/γ) (van Hagen et al., 1994). Other SS functions comprise vasoconstriction, antiproliferative actions in lymphocytes and inflammatory cells of the intestinal mucosa as well as in the cartilage and bone precursors.

1.1.3 Somatostatin receptors (SSTRs) structure

SS mediates its biological actions by binding to five subtypes of seven transmembrane domain G-protein-coupled-receptors (GPCRs), termed SSTR1-5 (Bruns et al., 1994; Patel, 1999). The SSTR subtypes can be classified into two groups, based on structural properties and pharmacological profiles. The first group includes SSTR2, SSTR3 and SSTR5 while SSTR1 and SSTR4 belong to the second group. Although they all bind SS-14 and SS-28 with high affinity, they display different affinity to SS analogs (SSAs). In particular, SSTR1 and SSTR4 do not bind octreotide and lanreotide, whereas SSTR2, SSTR5 and SSTR3 show high, moderate and weak affinity, respectively (Olias et al., 2004). The SSTRs are encoded by five genes localized on different chromosomes and the gene products have 42-60% sequence homology within different species (Patel et al., 1995). All SSTRs do not present introns in their coding sequences with the exception of sstr2, which contains one intron, thus two variants originate in rodents from mRNA alternative splicing: the unspliced form ($SSTR2_A$) and a shorter, spliced form ($SSTR2_B$), with smaller cytoplasmic tail. The long form of SSTR2 is the only one expressed in humans (Reisine & Bell, 1995; Patel, 1999). The protein structure of SSTRs comprise of 356 - 391 amino acids and show high sequence homology within transmembrane domains. In particular, the seventh domain contains the typical signal peptide (YANSCANPI/VLY) characteristic of this receptor family (Patel, 1999).

At the cytoplasmic side of the third transmembrane domain is located another conserved motif, the "DRY motif" (Asp-Arg-Tyr), which is necessary for G-protein coupling and inhibitory signal transduction. As recently demonstrated, the substitution of D136 and R137 residues in the DRY motif of SSTR5 resulted in the loss of the receptor ability to generate SS-mediated intracellular responses (Peverelli et al., 2009).

In contrast, SSTRs mostly differ in the N- and C- terminal sequence. Moreover, SSTRs present different N-linked glycosylation sites at the N-terminal, and a variable number of phosphorylation sites for protein kinase A, protein kinase C and calmodulin kinase II at the C-terminal, second and third intracellular loops (Patel et al., 1995).

1.1.4 SSTRs expression in the pituitary

All five SSTR subtypes are expressed in fetal and normal pituitary, whereas SSTR4 is almost undetected in the adult gland (Reubi et al., 2001; Neto et al., 2009; Ben-Shlomo & Melmed, 2010). The long variant of SSTR2 is the only form expressed in the human pituitary, whilst truncated SSTR5 variants have been detected in rodents as well as in humans, in normal and tumoral pituitary samples (Duran-Prado et al., 2009; Córdoba-Chacón et al., 2010). Binding studies revealed that the SSTR subtypes predominantly expressed in GH-secreting adenomas are SSTR2 and SSTR5 (expressed in more than 95% and 85% of tumors, respectively), followed by SSTR3 and SSTR1, both expressed in more than 40%; and finally SSTR4, which has rarely been found (Nielsen et al., 2001; Tabaoda et al., 2007). Due to its most abundant expression, SSTR2 has been pharmacologically targeted with SSAs to treat acromegaly. The following part of this chapeter will then focused on SSTR2, in particular in terms of signaling, internalization properties and new discovered molecular mechanisms underlying SSAs pharmacological resistance in patients harbouring GH-secreting adenomas.

1.1.5 SSTR2-mediated signal transduction

SS binding to SSTR2 leads to the activation of complex G-protein mediated signaling pathways, reflecting the pleiotropic effects of these receptor (Rens-Domiano & Reisine, 1992; Moller et al., 2003). G proteins are heterotrimeric molecules consisting of α, β and γ subunits. The α subunit determines the inhibitory or stimulatory nature of the G protein functional activity and contains the sites for GTP/GDP exchange. To date, 20 distinct α subunits have been cloned based on their structural homology and functions, and they have been divided in 4 groups: $G_{s\alpha}$, $G_{i\alpha}$, $G_{q\alpha}$, $G_{12\alpha}$. After ligand binding, a conformational change in the SSTR2 structure occurs, and the α subunit of G_i and G_q proteins are specifically recruited. The most characterized effects determined by G_i protein activation involve adenylyl cyclase activity inhibition, with resulting decrease in intracellular cAMP levels, and the modulation of ion channels (Patel et al., 1994). In fact, SSTR2 is directly coupled to potassium (K^+) channels, whose activation determines plasma membrane hyperpolarization. SSTR2 can modulate K^+ currents also in indirect manners, through the activation of phospholipase A2 and subsequent production of arachidonic acid, whose metabolites activate K^+ channels, or through the stimulation of phospholipase C (PLC) signaling pathway (Meyerhof, 1998). These events together with the closure of voltage-sensitive Ca^{2+} channels, reduce calcium (Ca^{2+}) influx and intracellular Ca^{2+} level, causing an impairment in the mobility of secretory vesicles, and the reduction of GH secretion in the pituitary (Ben-Shlomo & Melmed, 2010).

SSTRs control on cell proliferation is mediated by the stimulation of phosphotyrosine phosphatase (PTP) or mitogen-activated protein kinases (MAPK) activity (Ben-Shlomo & Melmed, 2010; Pan et al., 1992). Regarding SSTR2, its activation results in the coupling with PTP activation pathway involving the cytosolic Src homology 2 (SH2) domain, SHP1 (PTPN6), and SHP2 (PTPN11) and the membrane-anchored PTPη (DEP1) (Lopez et al., 1997). This, in turn, leads to growth factors kinases dephosphorylation, and the inhibition of mitogenic stimuli (Pages et al., 1999; Ferjoux et al., 2003), whereas SHP1-mediated nitric oxide synthase (NOS) dephosphorylation increases cGMP

levels and blocks cell proliferation (Bocca et al., 2000; Luque et al., 2005). SSTR2 negatively modulates the phosphatidylinositide-3-kinase (PI3K) target Akt (Bousquet et al., 2006) and inhibits ERK 1/2 activity with resulting ctitostatic effects (Sellers et al., 2000). Instead, cytostatic actions of SSTR5 seem to be PTP-independent but coupled to the PLC inhibitory pathway (Buscail et al., 1995). Moreover, SSTR5 inhibits the activity of several MAPKs: Ras (Cattaneo et al., 1999), Raf-1 (Cattaneo et al., 1996), c-fos (Cordelier et al., 1997) and ERK1/2 (Buscail et al. 1995, Peverelli et al., 2009). Both SSTR2 and SSTR5 activation up-regulates the cell cycle inhibitors $p27^{Kip1}$ and $p21^{Cip1}$ (Florio et al., 2001) which prevent the formation of the cyclin-dependent kinase (CDK) complexes, with consequent cell cycle arrest at the G1/S transition phase, as also reported in GH-secreting pituitary adenomas (Ben-Shlomo & Melmed, 2010).

SSTR2 and SSTR3 are the only SSTR subtypes that may initiate pro-apoptotic pathways. SSTR3-induced cell apoptosis involves p53 accumulation (Sharma et al., 1996), whereas SST2 was rather found to act through different mechanisms involving the down-regulation of mitochondrial Bcl-2 protein expression, and the up-regulation of the death receptors belongings to the TNF family (Teijeiro et al., 2002; Guillermet et al., 2003). In vitro experiments in tumoral cells from GH-secreting pituitary adenomas demonstrated that the SSTR2-mediated cytotoxic effects comprise the induction of the enzymatic activity of caspase-3 and the increase of cleaved cytokeratin (CK) 18 levels (Ferrante et al., 2006). Furthermore, in NIH-3T3 cells, SSTR2 was able to enhance the transcriptional activity of NF-kB and decrease JNK phosphorylation, causing cell apoptosis (Guillermet-Guiber et al., 2007).

A schematic representation of the main intracellular SSTR2-mediated signaling cascades are depicted in figure 3.

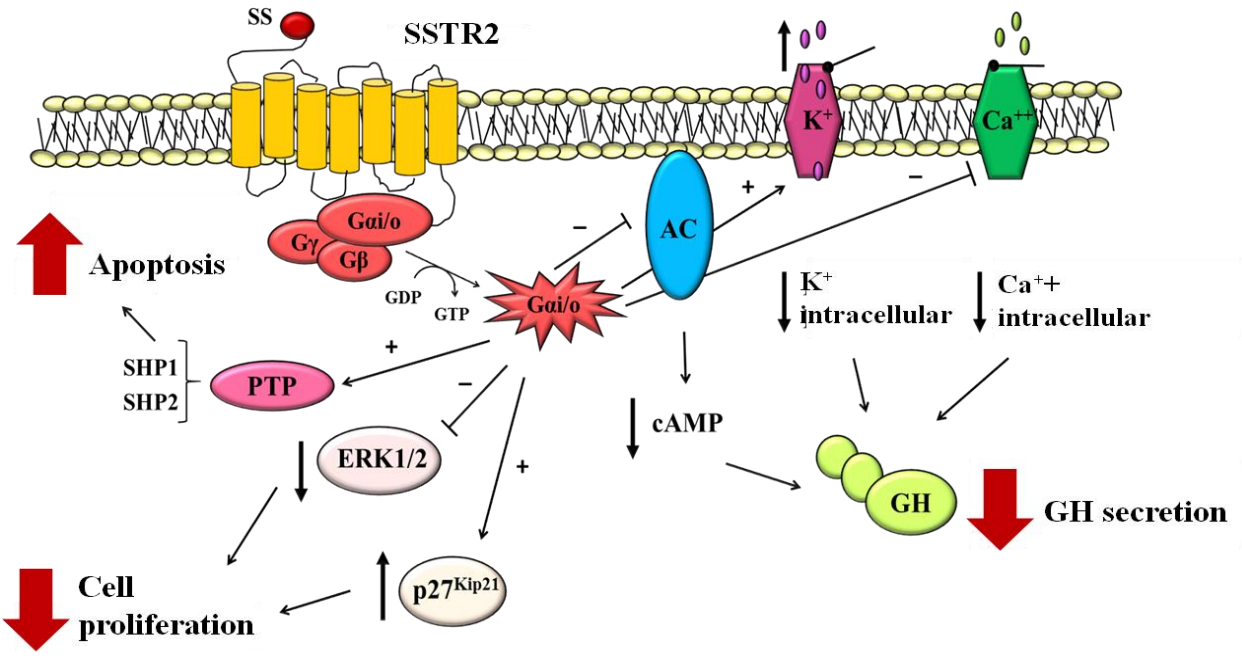

Figure 3. Schematic representation of the most important SSTR2-mediated intracellular pathways in GH-secreting cells. After SS binding, G_i proteins are activated and act to reduce adenylyl cyclase activity with consequent decrease in cAMP levels; this together with the modulation of ion channels, reduces the intracellular Ca^{2+} concentration to block GH release. Antiproliferative actions of SSTR2 include the activation of PTP, the inhibition of the MAPK, and the up-regulation of $p27^{Kip1}$ to arrest cell cycle in phase G1. SSTR2-dependent cytotoxic actions are mediated by the modulation of the expression of pro-apoptotic proteins.

1.1.6 Desensitization and internalization properties of SSTR2

The GPCR signaling cascade terminates when GTP/GDP exchange occurs on the α subunit of the G protein and GPCR kinases (GRKs) phosphorylate specific acceptor sites on the receptor. These phosphorylation events, followed by arrestins recruitment, support receptor desensitization by sterically disrupting GPCRs/G protein coupling (Kohout & Lefkowitz, 2003; Luttrell & Lefkowitz, 2002) thus preventing receptors from responding to further stimulation.

Experimental observations allowed to better characterize the molecular mechanisms involved in the regulation of SSTR2 desenstitization and internalization (Fig. 4). After few minutes oh hormone binding, several serine and threonine residues in the C-terminal tail of the human SSTR2 termed Ser341, Ser343, Thr353, Thr354, Thr356 and Thr359, become phosphorylated, (Nagel et al., 2011; Lehmann et al., 2014). GRK2 and GRK3 have been identified as major players in the agonist-

dependent SSTR2 phosphorylation, while PKA and PKC do not seem to be required (Hipkin et al., 2000; Pöll et al., 2010). Both nonvisual arrestins, β-arrestin-1 and β-arrestin-2, translocate to the plasma membrane where they bind to the phosphorylated receptor (Tulipano et al., 2004). β-arrestins have two sensor sites important for receptor interaction: a phosphate sensor that recognizes receptor-attached phosphates or negatively charged amino acids, and an activation sensor that binds receptor elements that undergo conformational modification upon activation (Gurevich et al., 2006). In order to mediate SSTR2 endocytosis, β-arrestins act as scaffold proteins for components of the endocytic machinery, such as clathrin, adaptor protein 2 (AP2) and phosphoinositides. Accordingly to the classification proposed by Oakley and co-workers, based on the agonist-induced arrestin-receptor binding properties, SSTR2 belongs to class B receptors (Oakley et al., 2000; Oakley et al., 2001). In fact, SSTR2 displays similar affinity of interaction for both β-arrestin-1 and 2, and it stably interacts with them. This thigh receptor-arrestin association allows the complex to internalize, via clathrin coated pits (Koenig et al., 1998), into endosomal vesicles as an unit (Oakley et al., 2001).

The internalized pool of receptors is then targeted to a perinuclear area resembling the Trans Golgi network (TGN) (Liu et al., 2005; Kao et al., 2011). After removal of ligand, most of the internalized receptor is rapidly dephosphorylated (Ghosh & Schonbrunn et al., 2011), and recycled to the plasma membrane (Tulipano et al., 2004) in contrast to what would be expected from a class B receptor. Finally, evidences from the literature showed that SSTR2 does not undergo any detectable lysosomal/proteosomal-induced degradation, since neither changes in SSTR2 ubiquitination level nor decrease of receptor expression have been reported even under prolonged stimulation protocols (Tulipano et al., 2004; Lesche et al., 2009; Peverelli et al., 2014).

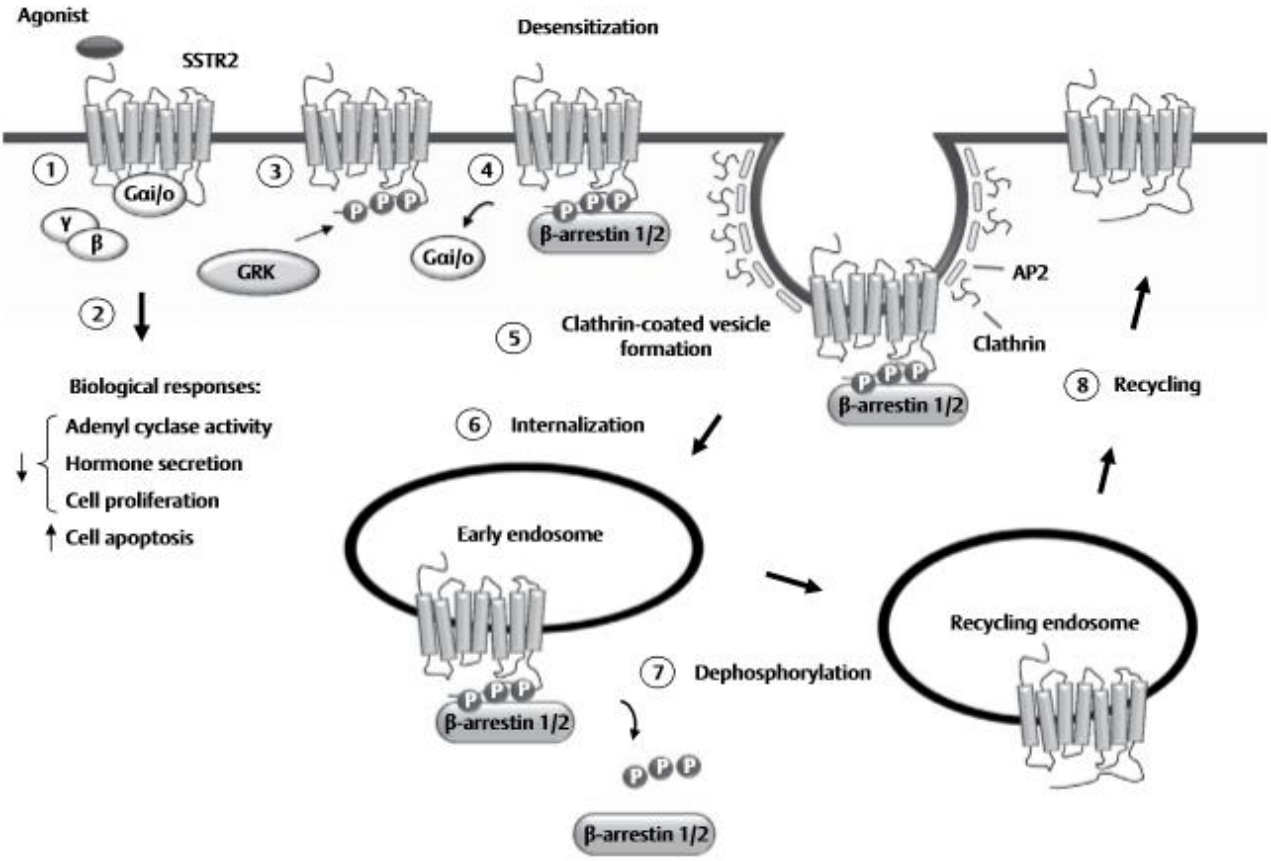

Figure 4. Agonist-mediated SSTR2 internalization scheme, from Treppiedi et al., 2016. Upon agonist binding SSTR2 activation results in the recruitment of Gi/o proteins (1) and the induction of biological responses (2). GRK-mediated phosphorylation of Ser and Thr residues located at the C-tail of SSTR2 terminates the signaling cascade. (3). β-Arrestin-1/2 bind to the phosphorylated receptor and sterically prevent its interaction with Gi/o proteins, thus determining SSTR2 desensitization (4). The complex SSTR2-β-arrestin is targeted to specific plasma membrane areas where clathrin and AP2 cooperate to assemble clathrin coated vesicles (5). Receptor and β-arrestin internalize together into early endosomes (6). β-arrestin dissociates from SSTR2 after receptor dephosphorylation that is in turn directed to the recycling pathway (7). SSTR2 reaches the cell surface where it can sustain another cycle of stimulation (8).

1.2 GROWTH HORMONE-SECRETING PITUITARY ADENOMAS

1.2.1 Growth hormone

Growth hormone (GH) is a 191 amino acid single chain protein released by anterior pituitary somatotroph cells. GH secretion occurs in pulsatile bursts, especially at night, with extremely low or undetectable levels occurring in the nadir between pulses, and is governed by secretory factors such as GHRH (growth hormone releasing hormone) and ghrelin, and by the inhibitory hypothalamic SS. Both these stimulatory and inhibitory factors are subjected to higher influences within the brain as well as to peripheral signals, therefore the overall secretion of GH can vary widely under different physiological conditions such as growth, fasting, stress and exercise (Frohman et al., 1992). The biological effects of GH are mediated directly through the GH receptor and include the control of skeletal growth, the regulation of glucose levels, protein and lipid metabolism. Moreover, one of the major protein induced by GH is represented by the insulin like growth factor1 (IGF-1), which primarily origins from the liver and acts to reduce insulin action and stimulate lipolysis, eventually exerting a negative feedback on GH release (Clemmons, 2004).

1.2.2 Acromegaly: epidemiology and aetiology

The pathological excessive secretion of GH, and consequently IGF-1, is associated with a rare but severe endocrine disorder known as acromegaly. Acromegaly occurs with an approximate incidence of 3-4 new cases per million of population per year with an estimated prevalence of 60 per million (Holdaway & Rajasoorya, 1999).

In more than 95% of cases the GH hypersecretion is due to a benign monoclonal pituitary adenoma which develops from the somatotroph cells that normally produce GH in the pituitary (Melmed et al., 1983). These somatotrophinomas are pure in 60% of cases, mixed GH- and prolactin (PRL)-secreting adenomas in 25% of cases, whereas very rarely they can co-secrete TSH or ACTH

(Bassetti et al., 1986; Socin et al., 2003). Pituitary carcinomas are extremely rare (less than 20 cases published in the literature) (Pernicone et al., 1997). Infrequently acromegaly is caused by ectopic secretion of GHRH from a peripheral neuroendocrine tumor (Thorner et al., 1984), or from abnormal hypothalamic GHRH secretion (Asa et al., 1984). About 5% of cases are associated with familial syndromes, most commonly multiple endocrine neoplasia type 1 (MEN1) syndrome, but also McCune Albright syndrome, familial acromegaly, Carney's syndrome and Familial Isolated Pituitary Adenoma (FIPA) (Horvath & Stratakis, 2008).

Both genders are equally affected and the diagnosis is typically made in adults aged 40 – 60 years. However, due to the insidious nature of onset of symptoms and slow progression there is usually a considerable delay (in the range of 4-10 years) in the establishment of the correct diagnosis. Younger patients often present a more aggressive disease related to more rapidly growing adenomas. Very rarely the disorder begins during childhood, thus resulting in gigantism.

1.2.3 Clinical description: symptoms and signs

In more than 70% of cases, GH secreting pituitary adenomas are large tumors (macroadenoma, $\geq$ 10 mm in diameter) which may present with local mass symptoms such as headache, visual field deficit or cranial nerve palsies, while microadenomas (< 10 mm in diameter) are less frequent. Defects of other anterior pituitary hormones secretion may also occur when the lesion increases in size. In fact, hypogonadism, presenting as decreased libido, infertility or oligo/amenorrhoea is a common finding at presentation and this may be due to both gonadotrophin deficiency as well as to hyperprolactinaemia, stalk compression or coexistent excessive secretion of prolactin (PRL), respectively (Greenman et al., 1995; Kaltsas et al., 1999). Patients with established acromegaly present a characteristic change in appearance comprising coarsening of the facial features: the nose is widened and thickened, the cheekbones are obvious, the forehead bulges, the lips are thick and the facial lines are marked. Mandibular overgrowth with prognathism, maxillary widening,

interdental separation and jaw malocclusion are typical signs of the disease as well as the enlargement of the hands and feet as reported in figure 5.

Figure 5. Some of the most evident clinical features of acromegalic patients: prognatism, enlargment of hands, interdental separation and jaw malocclusion. The patient gave his consent to the use of these pictures.

Generalised organomegaly is also commonly stated to occur in acromegaly (Molitch, 1992;). Accelerated degenerative changes particularly of the weight-bearing joints are a frequent occurrence leading to degenerative arthropathy (Stavrou & Kleinberg, 2001). Hypertrophy of the soft tissues of the upper airway and macroglossia that often result in obstructive sleep apnoea, represent other classical clinical manifestations, together with the reduced lung capacity that can turn in pulmonary complications (Grunstein et al., 1991). Acromegaly is also associated with decrease in fat mass, increase in lean body mass and muscle hypertrophy (Katznelson, 2009). Moreover, lipid metabolism alterations lead to the development of insulin resistance, hypertension and cardiomyopathy (Gama et al., 1997; Giustina et al, 2003), therefore, besides a considerable impairment of quality of life, uncontrolled patients have an increase in morbidity with an overall mortality at least two-fold that of the general population due to cardiovascular and cerebrovascular complications (Holdaway et al., 2004). In addition, it has become evident that patients with

acromegaly have an increased risk of developing neoplasia, particularly colon cancer (Renehan et al., 2003), whether the susceptibility to other malignancies remains controversial (Melmed, 2001).

1.2.4 Diagnosis: biochemical and radiological assessment

The diagnosis of acromegaly is made using a combination of clinical examination of the typical disfigurement of the patient and analysis of biochemical parameters. Patients with acromegaly have typically elevated serum GH concentrations, that are not suppressed to a level < 0.4 ng/ml following an oral glucose load (oral glucose tolerance test, OGTT) (Ben-Shlomo & Shlomo, 2008). Measurement of serum GHRH may be performed in the rare patients in whom a non-pituitary aetiology is suspected. A skull x-ray represents a quick and easy preliminary assessment for the confirmation of the disease, even though more detailed information regarding the presence and size of a pituitary mass requires a computed tomography or, better, an MRI contrast enhanced scan, as shown in figure 6. Neuro-ophthalmological assessment is obligatory in all cases of acromegaly and assessment of the integrity of the other pituitary hormones needs to be performed by a combination of the appropriate basal and dynamic tests.

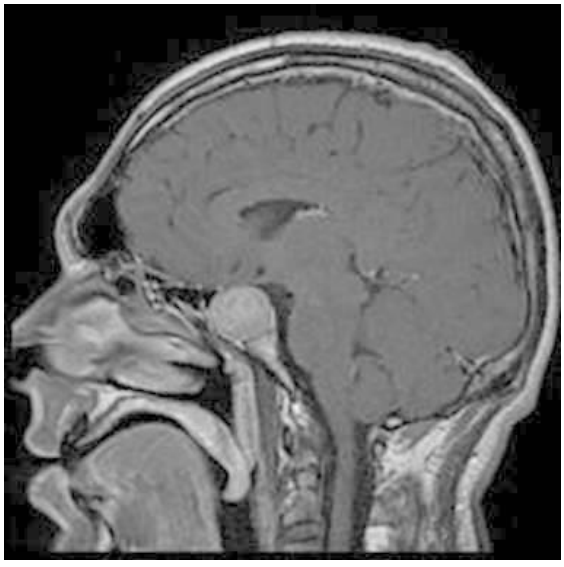

Figure 6. MRI image indicating a GH-secreting pituitary macroadenoma.

1.2.5 Management and treatment

The clinical aims for acromegaly are: to relieve symptoms, to reduce the volume of the pituitary tumor, to prevent the recurrence, and to improve long-term morbidity and mortality. The control of the disease is achieved when GH concentration returns below 2.5 μg/l or GH nadir after 75g OGGT less than 1.0 μg/l and IGF-I level returns in the normal range adjusted for age and gender (Giustina et al., 2000). A stepwise therapeutic approach using surgery and/or radiotherapy and/or medical treatment allows to satisfy these goals.

Currently, trans-sphenoidal surgery is the initial treatment of choice for the majority of patients. With modern equipment and experienced surgeon, it is a safe procedure with a low complication rate and mortality of less than 0.5%. In the last decades, surgical techniques have included the use of intra-operative MRI (Fahlbusch et al., 2005) and intra-operative growth hormone measurement (Abe & Ludecke, 1999), while the development of endoscopic trans-sphenoidal surgery has been reported to offer several advantages in terms of superior tumor clearance, especially suprasellar extension, less surgical morbidity, fewer complications, and reduced post-operative discomfort (Frank et al., 2006). The major long-term complication associated with trans-sphenoidal surgery is worsening of anterior pituitary function and hypopituitarism (Sheaves et al., 1996). Others minor complications include diabetes insipidus, cerebral spinal fluid (CSF) rhinorrhoea and the syndrome of inappropriate antidiuretic hormone secretion (SIADH). Surgical outcome is carefully assessed at three months. When surgery fails to achieve a good disease control, or when surgery is impossible or contraindicated, patients are offered radiotherapy and/or pharmacological treatments.

Radiotherapy in this setting is usually external and centered on the tumor; an average total dose of 50 Gy is delivered in about twenty five daily sessions. Highly focused irradiation (radiosurgery, stereotactic radiotherapy, "gamma-knife", etc.) is now available in some centres, and causes less damage to neighbouring tissues. 10–15 after irradiation, a variable degree of anterior pituitary insufficiency has been reported in 80% to 100% of patients. Complications including radionecrosis

and optic neuropathy are now very rare. On the other hand, the risk of stroke may be increased, sometimes many years after radiotherapy (Brada et al., 1999).

Regarding the medical therapy, three different types of drugs are currently available in the clinical practice: SSAs, GH antagonists and dopamine agonists.

The potent antisecretory and antiproliferative properties of SSTR and the identification of the key molecular structural characteristics of SS, provided the basis for the development, in the mid-1980's, of specific ligands which represented the real therapeutic advance for acromegaly. Octreotide (Sandostatin, Novartis, Basel, Switzerland), the 8 amino acid synthetic somatostatin analog, was the first compound to be marked (Bauer et al., 1982). This SSA showed a considerable increase of half-life compared to the native SS (approximately 90-seconds), and its administration subcutaneously in a thrice-daily regimen resulted in stable drug concentrations and maximal effects. GH concentration reduction was seen in more than 90% of patients, with approximately 50-60% achieving levels of less than 2 ng/ml and a normal serum IGF-1 level. Currently, octreotide is not used anymore for chronic treatment in acromegalic patients, since long lasting formulations of SSAs have become available. These formulations contain a biodegradable polylactide and polyglycolide polymers from which the active drug is released after intramuscular injection. There are three such preparations available, octreotide LAR (Sandostatin LAR, Novartis) which has high affinity for SSTR2 and moderate and weak affinity for SSTR5 and SSTR3 (McKeage et al., 2003), respectively, is given at a variable dose of 10 mg, 20 mg or 30 mg at recommended four weekly intervals; lanreotide (Somatuline Autogel, Ipsen Biotech, Paris, France), which acts as a selective agonist of SSTR2 and SSTR5, is given as a single dose of 60-120 mg every 28 days as a sub-cutaneous depot formulation (Castinetti et al., 2009); and the recently licensed pasireotide LAR (SOM230) which displays increased affinity for SSTR5, but is also selective for SSTR2 and SSTR3, and shows enhanced binding to SSTR1 compared to octreotide (Bruns et al., 2002; Lewis et al., 2003).

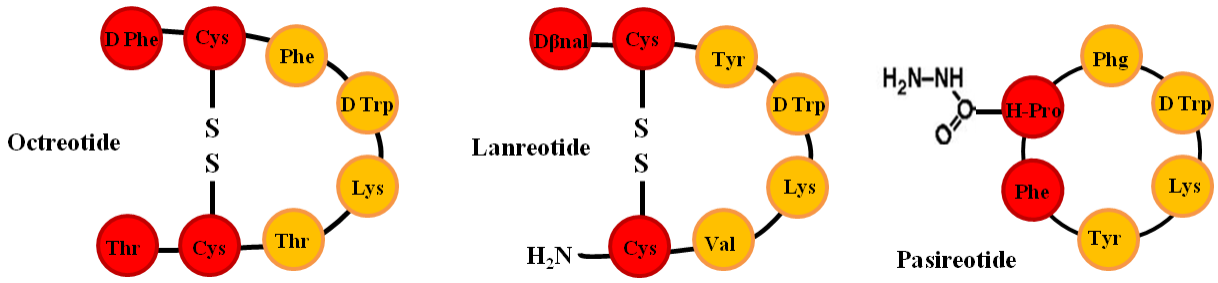

Figure 7. Amino acid sequences of three somatostatin receptor ligands, octreotide, lanreotide and pasireotide.

Another therapeutic approach to decrease GH level in acromegalic patients is represented by pegvisomant, the new genetically engineered growth hormone molecule that acts by binding peripheral GH receptors, preventing receptor dimerization and subsequent signal transduction, and blocking IGF-I synthesis (Berryman et al., 2007). This GH receptor antagonist is the major advance in the treatment of acromegaly with several studies demonstrating its effectiveness and long-term efficacy (Trainer et al., 2000). However its role as first line option remains to be determined and to date it is mostly used for patients with proven resistance to long-term high-dose SSAs treatment after unsuccessful surgery and/or radiotherapy (Colao et al., 2006). The main drawbacks of pegvisomant are its daily injection requirement, and its high cost, thus it is not yet universally available.

Dopamine agonists (DA), such as bromocriptine and cabergoline, are ergot-derived dopamine analogs selective for the dopamine receptor type 2 (DRD2). These compounds were used as the sole pharmacological treatment for acromegaly until the introduction of SSAs. Although approximately 80% of patients showed a decrease in GH levels after treatment with bromocriptine, only about 10-15% achieved a complete control (Wass et al., 1977). Furthermore, bromocriptine attenuated moderately the symptoms and the reduction in tumor size was insignificant. Cabergoline, instead, offered greater advantages and appeared to be more effective (Sandret et al., 2012), and it is currently used in combination with SSAs (Cozzi et al., 2004).

1.2.6 Resistance to SSAs

According to published reports, about one third of patients receiving the medical therapy displays resistance to SSAs and fails to obtain a complete control of the disease (Ben-Shlomo & Melmed 2008; Melmed et al., 2009; Fleseriu, 2013). Resistance to SSAs can be defined as: 1) persistent basal GH excess associated to GH nadir greater than 1.0μg/liter after OGTT and IGF-I levels above the normal range adjusted for age and gender, known as the "biochemical resistance"; and 2) increase in tumor size or a tumor shrinkage less than 20% compared with baseline volume, known as the "tumor resistance" (Gola et al., 2006).

The molecular mechanisms underlying the variable sensitivity of GH-secreting pituitary adenomas to SSAs have been extensively investigated over the past years, and three main hypotheses have been raised to explain this biological phenomenon:

1. impairment or heterogeneity of SSTR within the tumors, or decrease density of the SSTR subtypes with higher affinity to SSAs;
2. SSTRs gene mutations;
3. post-receptor alterations.

2.5.1 Alteration of SSTRs expression

The first hypothesis is the most investigated and supported by good evidence showing a reduced density of SSTR, especially SSTR2 and/or SSTR5 in GH-secreting adenomas from resistant patients. A significant correlation between the absence of SSTR2 expression and the poor hormonal response to SSAs has been reported in vivo (Plöckinger et al., 2008). Accordingly, Reubi and Landolt showed that a quantitative loss of SSTR accounted for the reduced sensitivity or resistance of a group of GH-secreting pituitary tumors in response to acute administration of somatostatin or octreotide (Reubi & Landolt, 1989). Moreover, SSTR2 expression resulted positively correlated with SSAs response, at both mRNA and gene product

levels (Taboada et al., 2008). In addition, another independent study demonstrated the existence of a positive association between SSTR2 expression, at a protein level, and in vitro GH suppression or in vivo IGF-I control (Ferone et al., 2008). A recent study performed with monoclonal anti-SSTR2 antibody immunostaining of paraffin-embedded tissues predicted SSAs responsiveness in acromegalic patients (Brzana et al., 2013).

However, such a loss of SSTR2, is not always found in resistant patients and cannot give an exhaustive explanation for the partial GH-suppressive effects of SSAs. Therefore, some studies focused on SSTR5, the other SSTR subtype widely expressed in GH-secreting tumors, correlating the resistance of a group of GH-secreting pituitary adenomas to SSAs with an absent or reduced density of SSTR5 (Gadhela et al., 2013). Moreover, there are observations highlighting the synergic effect on GH secretion resulting from the activation of SSTR2 and SSTR5 (Tulipano et al., 2001), and evidence showing enhanced functionality of SSTR2/SSTR5 heterodimers (Rocheville et al., 2000; Grant M; et al., 2008). The altered heterogeneity of SSTRs pattern within the tumor may be related to the pharmacological resistance to SSAs. In this regard, a study performed on a series of resistant GH-secreting adenomas revealed the lack of a homogeneous distribution of the SSTRs with high affinity for SSA (Reubi et al., 1987). This led to the hypothesis that a weak sensitivity to SSAs might be linked to the outgrowth of tumor cell clones still expressing SSTRs, but those subtypes for which SSAs display low affinity, thus explaining the basis of the secondary development of resistance. Altogether these works support the thesis of a key role of SSTR2 and SSTR5 expression in the development of a variable sensitivity to SSAs.

2.5.2 Mutations in SSTR genes

As reported in the literature, gene mutations leading to a loss of function in SSTR were rarely found in patients bearing GH secreting adenomas, suggesting that this hypothesis cannot actually be at the basis of pharmacological resistance to SSAs (Petersenn et al., 2000; Corbetta

et al., 2001). To date, the only known germ line mutation (R240W) in the SSTR5 gene was found by Ballarè and colleagues in a patient with a GH secreting adenoma resistant to SSAs treatment (Ballarè et al., 2001): this missense mutation resulted in reduced inhibitory effect of SS on GH release and cell growth. In vitro experiments in GH3 cells showed that the mutant R240W receptor maintained its ability to decrease adenylyl cyclase activity but lost the inhibitory action on GH secretion as a consequence of a lack of coupling with G_{oA} protein but not with the other G proteins activated by wild type SSTR5, for example, G_{i1}, $_{i2}$, $_{i3}$ and G_{oB} (Peverelli et al, 2009; Peverelli et al., 2013). Moreover, in CHO cells transfected with the mutated receptor, the antiproliferative effect of SS resulted reverted, as demonstrated by an increase in the MAPK activity compared with wild-type cells (Peverelli et al., 2009)

Several studies evaluated the presence of polymorphisms in SSTR2 and SSTR5 genes in a large series of patients with acromegaly, eventually attempting to correlate them to the sensitivity to SSAs. However, none of the described polymorphic variants in SSTR2 and SSTR5 (t80c, c-57g, and a-83g in SSTR2, t-461c and c1004t in SSTR5) seem to play a major role in determining SSAs resistance (Filopanti et al., 2005; Lania et al., 2008). Conversely, the truncated variants of SSTR5 (SSTR5TMD4) has been correlated with resistance to octreotide and tumor invasive behavior in SSTR2 expressing GH-secreting adenomas (Durán-Prado et al., 2010; Luque et al., 2015). The dominant-negative effect of SSTR5TMD4 on SSTR2-mediated signaling has been demonstrated by different approaches, and SSTR2-SSTR5TMD4 interaction was found responsible for the reduced SSTR2 responsiveness to SS (Durán-Prado et al., 2012) likely by altering the normal SSTR2 trafficking to the plasma membrane (Durán-Prado et al., 2009).

2.5.3 Post-receptor alterations

In attempt to understand the molecular mechanisms underlying the pharmacological resistance to SSAs, many studies focused on post-receptor alterations involving the intracellular signaling molecules directly activated by SSTRs. The decreased sensitivity of SSTRs to SSAs may be in

fact related to receptor uncoupling with the transduction system, and pharmacological resistance may affect distinct SS-induced intracellular pathways, as documented in rare cases of non-responder acromegalic patients in which the resistance selectively involved the antisecretory effects or the antiproliferative actions of SSAs (Casarini et al., 2006; Resmini et al., 2007).

Few data are available regarding G proteins alterations as possible determinants of pituitary tumor resistance to SSAs (Ballarè et al., 1997). However, it is worth nothing that about 30-40% of acromegalic patients carry somatic activating mutations in the gene coding for the α subunit of G_s proteins (GNAS, also known as gsp oncogene). This mutation is associated with elevated basal adenylyl cyclase activity, poor responsiveness to GHRH, and higher sensitivity to SSAs, a characteristic that still lacks of an explanation since no increase in SSTRs expression have been reported in these adonomas (Spada et al., 1990; Barlier et al., 1999).

Genetic alterations in aryl hydrocarbon receptor interacting protein (AIP) seem to play a role in SS-resistance of non familial acromegalic patients. AIP is considered a tumor-suppressor gene that, acting through ZAC, is able to induce tumor shrinkage (Chahal et al., 2012). In addition, AIP inactivation has been demonstrated to affect G_i signaling and induce pituitary tumorigenesis (Tuominen et al., 2015). Indeed, genetic analysis on 50 sporadic GH-secreting adenomas classified as not responder to SSAs revealed the presence of a low prevalence of germline mutations in AIP gene (Oriola et al., 2012).

The antiproliferative effects of SS are in part mediated by the MAPK pathway. Alteration in this signaling cascade, in particular regarding the expression level of Raf kinase inhibitory protein (RKIP), has been to found to affect the responsiveness of GH-secreting adenomas to SSAs (Fougner et al., 2008), as well.

Lately, it has been hypothesized that alterations in β-arrestins recruitment or in the arrestins expression levels could play a role in SSTR desensitization, internalization and trafficking,

thus modulating the response to SSTR-targeting drugs in GH-secreting pituitary adenomas. Peverelli and colleagues demonstrated that the previously mentioned naturally occurring missense mutation R240W, located in the third intracellular loop of SSTR5, strongly impaired receptor agonist-induced phosphorylation, arrestin interaction, and receptor internalization (Ballarè et al., 2001; Peverelli et al., 2008), with important consequences on receptor signaling (Peverelli et al., 2009; Peverelli et al., 2013). Recent findings from another work negatively correlated β-arrestin-1 mRNA expression with the reduction of GH levels in acromegalic patients after acute octreotide stimulation (Gatto et al., 2013). In addition, low β-arrestin-1 and 2 mRNA expression and high GRK2 and SSTR2 mRNA levels have been detected in adenoma samples deriving from patients in which GH secretion was well inhibited by octreotide administration with respect to the resistant group (Gatto et al., 2016). Therefore, altered β-arrestins-SSTR2 interaction might eventually affect the rate of SSTR2 recycling and availability at the cell surface, thus determining a reduced in vivo responsiveness to SSAs.

Filamin A (FLNA), a recently discovered modulator of SSTR2 expression and signaling in GH-secreting adenomas, further validated the hypothesis of post-receptor alterations as possible causes for the pharmacological resistance to SSAs. The role of FLNA will be discussed in detail in the following chapter of the present thesis.

1.3 FILAMIN A

1.3.1 FLNA structure

The mammalian Filamins belong to a family of large actin binding proteins comprises of three members: FLNA, B and C, with a high homology in their coding sequence (van der Flier & Sonnenberg A, 2001). Specifically, FLNA, mapping to Xq28, is the most expressed isoform in human adults and was the first actin binding protein discovered in non muscle cells (Hartwig and Stossel, 1975). Human genetic diseases associated with FLNA mutations have been described, such as the X-chromosome-linked brain malformation known as periventricular nodular heterotopia (PVNH), otopalatodigital syndrome (OPD), frontometaphyseal dysplasia (FMD), and Melnick Needles syndrome (MNS) (Robertson et al., 2003).

FLNA structure is characterized by the self-association of two monomers of 280 kDa each. Each subunit has an actin-binding domain (ABD) localized at the N-terminal containing two calponin-homology domains CH1 and CH2, followed by 24 immunoglobulin (Ig)-like repeats of about 96 amino acid residues fold into antiparallel β-sheets. The first calpain-sensitive hinge region (H1) separates the repeats in 2 rod domains (Rod-1 and Rod-2). Rod-1 (repeats 1–15) contains a secondary actin binding domain with lower affinity, while Rod-2 (repeats 16–23) has a more globular structure and function as interface for intracellular factors interaction (Nakamura et al., 2011). The second hinge region divides Rod-2 from the repeat 24, at the C-terminal, which represents the region of dimerization that confers to FLNA a V-shaped flexible arrangement. A schematic representation of FLNA is depicted in the figure 8.

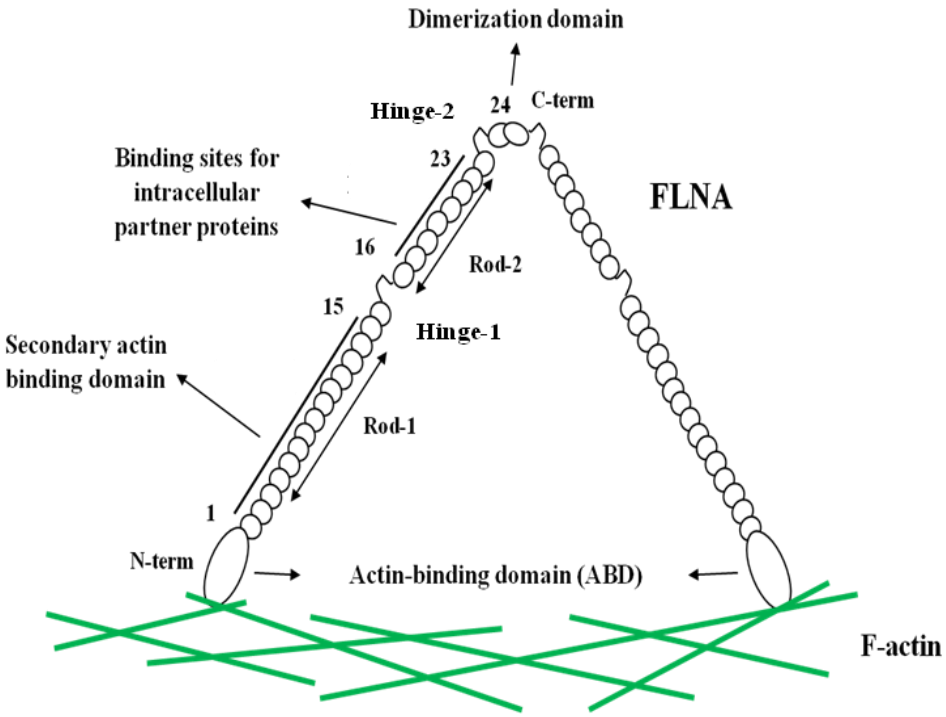

Figure 8. Illustrative image of FLNA structure. The main actin binding domain is located at the N-terminal, followed by 24 repeats Ig-like, divided by the first hinge region in two rod domains: Rod 1 (repeats 1-15) and Rod-2 (repeats 16-23). The second hinge region separates the repeat 23 from the repeat 24. The monomers self-association site is located at the C-terminal and FLNA dimerization promotes orthogonal junctions of F-actin.

1.3.2 FLNA biological functions

The biological functions of FLNA relies on its proteic structure. Infact, thanks to its extended filamentous structure, the main FLNA action is to cross-link F-actin into perpendicular branchings and form a cytoskeleton network in order to maintain the physiological cell shape. Moreover, FLNA orchestrates the engineering of the actin cytoskeleton in response to extracellular chemotattic stimuli. Another FLNA function is to physically anchor transmembrane proteins (GPCRs, ion channels, integrins) to the cortical actin structures (Stossel et al., 2001), thus regulating their localization and stability at the plasma membrane. FLNA also acts as a scaffold protein for signal transduction, by interacting with several cytosolic molecules such as kinases and transcription factors (Nakamura et al., 2011). Some of FLNA binding proteins are indicated in the figure below (figure 9).

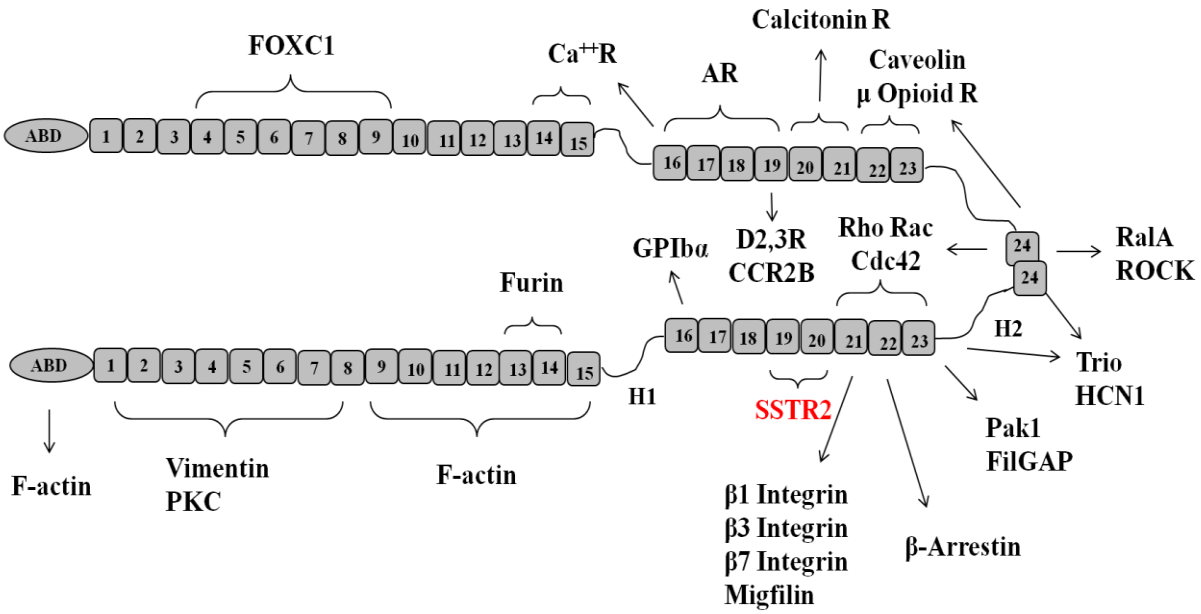

Figure 9. Schematic representation of FLNA interaction sites for partner proteins.

Furthermore, several data support the idea of FLNA as a key modulator of internalization and intracellular trafficking of transmembrane proteins. To this regard, FLNA has been recently demonstrated to actively coordinate DRD2 targeting to the cell surface in pituitary tumoral lactotrophs cells (Peverelli et al., 2012), promote DRD3 internalization (Lin et al., 2001; Cho et al., 2007) and direct surface HCN1 channels into endosomes in hippocampal neurons (Noam et al., 2014). In addition, FLNA and caveolin-1 interaction resulted involved in the clustering and lateral mobility of caveolae at the plasma membrane and responsible for the enhanced caveolae internalization in endothelial cells (Muriel et al., 2011). Cytokine receptor 2B (CCR2B) requires FLNA for clathrin coated pits formation and subsequent endocytosis (Minsaas et al., 2010). Further evidence showed that agonist-induced μ-opioid receptor internalization and intracellular trafficking are both positively supported by FLNA (Onoprishvili et al., 2003), whereas FLNA protects the calcitonin receptor (Seck et al., 2003), the calcium sensing receptor (Zhang & Breitwieser, 2005) and the cystic fibrosis transmembrane conductance regulator and the high-affinity IgG receptor FcRI (Thelin et al., 2007; Beekman et al., 2008) against degradation. Altogether these results

pointed out the pleiotropic role of FLNA in the organization of cellular compartments and directing protein traffic. All FLNA actions are regulated by phosphorylation events, proteolysis, mechanical forces, and multimerization with different partners.

1.3.3 Role of FLNA in the regulation of SSTR2 and impact on pharmacological resistance of GH-secreting adenomas

A recent published work showed that FLNA directly binds SSTR2. This FLNA-SSTR2 interaction was detected by surface plasmon resonance and involves the first intracellular loop of SSTR2 and FLNA repeats 19–20.

FLNA coupling to SSTR2 resulted crucial to sustain the SSTR2 antiproliferative effects in pancreatic tumor cells BON and in melanoma cell lines. Moreover, the authors demonstrated that FLNA stabilizes SSTR2 at the plasma membrane after ligand binding and regulates its endocyotosis rate (Najib et al., 2012).

In a following study, FLNA has been identified as a possible candidate for the determination of the pharmacological resistance to SSAs of GH-secreting pituitary adenomas (Peverelli et al., 2014). The more relevant results of the study concerned the functional role of FLNA in the regulation of SSTR2 signaling in tumoral somatotrophs as well as in a rat pituitary GH-secreting cell line GH3. In fact, FLNA supported SSTR2 effects on cell proliferation inhibition and on cell apoptosis induction. Moreover, in downregulation experiments, FLNA resulted crucial to prevent SSTR2 lysosomal degradation, thus stabilizing the receptor expression. This evidence has been demonstrated in GH3 cells overexpressing a FLNA dominant negative mutant that selectively avoids FLNA-SSTR2 interaction (FLNA repeats 19–20), with SSTR2 expression resulting significantly reduced after 72 h of agonist treatment. Furthermore, a FLNA fragment containing the repeats 21-24 of FLNA was used to generate a dominant negative for FLNA scaffold functions, since these repeats represent the region of FLNA mainly involved in the interaction with

intracellular partner proteins. Indeed, the overexpression of this truncated mutant strongly impaired the cytotoxic and cytostatic effects of SSTR2 in GH3 cells, suggesting that the FLNA scaffold function is necessary for the assembly of signal transduction complexes SSTR2-activated. Finally, although no correlation between FLNA and SSTR2 have been detected at the protein level and no effect on receptor localization have been observed after FLNA silencing in GH secreting adenomas samples, altogether these data support the hypothesis that low levels of FLNA might correlate with the poor response to SSAs in GH-secreting pituitary tumors still expressing SSTR2.

Similar effects of FLNA on the regulation of DRD2 have been obtained in PRL-secreting pituitary adenomas, thus confirming the crucial role of this protein in modulating the responsiveness of different pituitary tumors to the medical therapy (Peverelli et al., 2012). Moreover, in a recent study Vitali and collegues also demonstrated that FLNA is essential for SSTR2 expression, signaling and internalization in pancreatic neuroendocrine tumors (P-NET) (Vitali et al., 2016).

2. AIM OF THE STUDY

SSTR2 is one of the most expressed SSTR subtypes in GH-secreting pituitary adenomas and currently represents the main pharmacological target to treat acromegalic patients with somatostatin analogs (SSAs). However, the complete control of the disease is achieved in only two thirds of patients undergoing medical therapy, with a consistent subset of resistant cases. Recently, increasing attention has been focused on SSTR2-post receptoral alterations as possible molecular mechanisms underlying the biological phenomenon of drug resistance.

In this contest, FLNA, a large cytoskeleton protein with scaffold functions, has been pointed out as a new modulator of agonist activated-SSTR2 response and stability at the plasma membrane in GH-secreting cells. It is well known that cytoskeleton elements are able to mediate the formation of specialized domains at the plasma membrane, where cell surface receptors are assembled into functional units essential for the intracellular signaling transduction, and are involved in ligand-promoted receptor endocytosis, eventually regulating the amount of active receptor. However, to date there are no data in the literature describing the dynamic of SSTR2/FLNA interaction at the plasma membrane *in vivo*.

Therefore the aims of the present study were to get insights into the SSTR2 behavior at the cell surface before and after agonist stimulation, to evaluate the spatial arrangement of FLNA-SSTR2 complexes and the possible involvement of FLNA in regulating SSTR2 mobility and agonist-triggered clusters formation.

One of the most useful ways to study the formation of protein complexes and the occurrence of protein-protein interactions at the cell surface is to monitor their movements. SSTR2/FLNA interactions were analyzed at single-molecule level by single-molecule imaging, a powerful tool for the characterization of dynamic processes with high spatial and temporal resolution.

Moreover, we aimed to characterize the impact of the disrupted SSTR2/FLNA interaction on the anchorage of SSTR2 pits to the actin cortical cytoskeleton, and on the overall SSTR2 internalization process.

3. MATERIALS AND METHODS

3.1 Plasmids and Constructs

Plasmid encoding human SSTR2 was kindly provided by Dr. Stefan Schulz (Institute of Pharmacology and Toxicology, Jena University Hospital, Friedrich-Schiller-University, Jena, Germany). SNAP-tagged SSTR2 construct was cloned by fusing the N-terminus of the wild-type receptor to the SNAP sequence into a pcDNA vector, where the SNAP tag is located directly after the FLAG sequence (Calebiro et al., 2013). SNAP-tag is a 20 kDa peptide derived from the enzyme O^6-alkylguanine-DNA-alkyltransferase (AGT) that can be covalently labeled with synthetic dyes linked to benzylguanine (BG) allowing the visualization of the fused protein of interest.

Plasmid CLIP-tagged FLNA was generated by replacing EGFP with CLIP-tag in the construct coding for FLNA-EGFP (Planagumà et al., 2012) kindly provided by Dr. Anna M. Aragay (Institut de Biologia Molecular de Barcelona, Spain), with CLIP-tag introduced in the first hinge region of the FLNA monomer. CLIP-tag is a further engineered peptide that can be efficiently labelled with benzylcytosine derivatives.

FLNA truncated mutants constructs, containing the FLNA repeats 19-20 and 17-18 (FLNA 19-20, FLNA 17-18) used to prevent SSTR2/FLNA interaction and as a control, respectively, were previously described (Peverelli et al., 2014). Indeed, the repeats 19-20 of FLNA were demonstrated to interact with the first intracellular loop of SSTR2 *in vitro* (Najib et al., 2012). The N-terminus of these FLNA fragments were fused with the dsRed protein, allowing the monitoration of the transfection efficiency at a fluorescence microscope and resulting in a stabilized expression of the short peptides.

Lifeact-GFP was used as a marker for the visualization of F-actin in living cells after transfection.

3.2 Cell Culture

Chinese hamster ovary K1 (CHO-K1) cells were maintained in Dulbecco's modified Eagle's medium/nutrient mixture F-12 (DMEM/F12) supplemented with 10% (v/v) Fetal Bovine Serum (FBS), 100 U/ml penicillin and 100 µg streptomycin. Human melanoma cell line M2 (lacking expression of FLNA) and isogenic cell line A7 (stably expressing full-length FLNA) were kindly provided by Dr. Fumihiko Nakamura (Harvard Medical School, Boston, MA, USA) and cultured in α-minimal essential medium (MEM) supplemented with 8% (v/v) newborn calf serum (NBCS), 2% (v/v) FBS, and antibiotics. A7 cells were cultured in the presence of 500 µg/ml G418. Human Embryonic Kidney 293 (HEK293-AD) cells were grown in Dulbecco's modified Eagle's medium (DMEM) supplemented with 10% (v/v) FBS, 2mM glutamine, and antibiotics. Cells were maintained in a humidified atmosphere of 5% CO_2 at 37 °C.

3.3 cAMP Measurements

To confirm the functional activity of SNAP-tagged SSTR2 in terms of cAMP inhibition ability, HEK293-AD cells were transiently cotransfected for 48 h with 1µg of the wild-type or SNAP-tagged SSTR2 and 1 µg of the Epac1-camp sensor using the Effectene reagent (QIAgen, Hilden, Germany), according to the instructions of the manufacturer.

The construct coding for the cAMP sensor comprises of a cAMP-binding domain, derived from the exchange protein directly activated by cAMP (Epac), flanked on each side by CFP either YFP. Forskolin-triggered intracellular cAMP levels were recorded before and after incubation with increasing concentration of the selective SSTR2 agonist BIM23120 (Ypsen, Milan, IT), by Fluorescence Resonance Energy Transfer (FRET) measurements, following the previously described protocol (Nikolaev et al., 2004). In our settings, the inhibition of cAMP accumulation SSTR2-mediated results in a reduced binding of cAMP molecules to the Epac1-camps determining

a conformational change so that the distance between the CFP and YFP decreases causing an increase of FRET ratio. Ratiometric FRET experiments were performed on a Zeiss Axiovert 200 inverted microscope equipped a polychrome V light source a beam splitter and a CoolSNAP HQ CCD Camera. Graphpad Prism 5 software was used to plot in a logarithmic scale data from 10 cells for each group from three independent transfections.

3.4 Single-Molecule and Total Internal Reflection Fluorescence Microscopy

Single-molecule imaging is a strategy which combines the labelling of SNAP/CLIP-tagged proteins with small organic fluorophores and the use of a total internal reflection fluoresence (TIRF) microscope to unreveal their dynamics and heterogeneous behaviors on the surface of living cells. The low penetration depth (maximum ~200nm) obtained with TIRF microscopy allows to strongly reduce the background fluorescence and makes the technique particularly suited to study biological events occurring at the plasma membrane. An illustrative picture of the method is shown in figure 10.

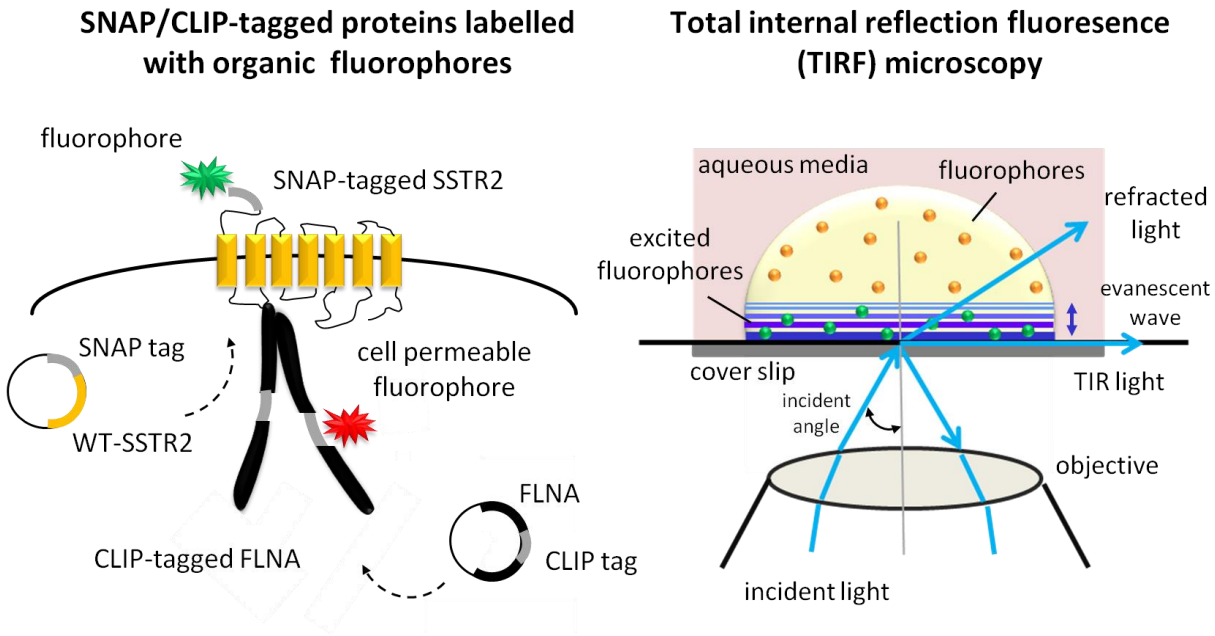

Figure 10. Single-molecule imaging requires low expression levels of SNAP/CLIP tagged proteins labeled with small, bright organic dyes. The visualization of distinct particles at the plasma membrane of living cells is performed with a TIRF microscope. The concept of TIRF microscopy relies on the physical phenomenon of the total internal refraction light (TIR). TIR occurs when the incident angle of the excitation light beam at the coverslip is greater than the 'critical

angle' so that the light is totally reflected back towards the objective lens and a thin electromagnetic field, known as the evanescent field, is generated at the interface. Only fluorophores located at the cell surface can be excited and detected.

For single-molecule experiments, CHO cells and melanoma cells were seeded on 24-mm clean glass coverslips at a density of 3 and 4,5 × 10^5 cells per well, respectively, in complete phenol-red-free medium in order to minimize autofluorescence. Indeed, extensive coverslips cleaning is essential to reduce the background fluorescence. The procedure consists of two consecutive incubations with chloroform and 5M NaOH, respectively, in a bath sonicator for 1 h each. The day after plating, cells were transiently transfected with 2 μg of total amount of DNA and 4-6 μL of Lipofectamine 2000 transfection reagent (Invitrogen, Carlsbad, CA), according to the instructions of the manufacturer. Cells were analyzed 4–12 h after transfection to achieve low expression. CHO cells, M2 and A7 cells transfected with SNAP-tagged SSTR2 were labeled with 1 μM Alexa647-BG (Alexafluor 647-SNAP Surface; New England Biolabs, UK). CHO cells also expressing CLIP–tagged FLNA were labeled with 1 μM BC-TMR (CLIP-Cell TMR-Star; New England Biolabs, UK), as well. The labeling was performed in complete phenol-red–free medium for 20 min at 37 °C 5% CO_2. At the end of the incubation, cells were washed three times with complete phenol-red–free medium, each time followed by 5 min incubation at 37°C, and immediately imaged. These conditions resulted in optimized labeling of cell-surface SNAP-tagged receptors and intracellular CLIP-tagged FLNA particles.

A custom total internal reflection fluorescence (TIRF) microscope (Eclipse Ti, Nikon) equipped with four EM-CCD cameras (iXon3+ DU897D-CSO, Andor), and a 100× oil-immersion objective (CFI Apo TIRF 100x/1.49, Nikon) was used. Cells were first searched and focused using bright field illumination, then a fine focus adjustment was performed switching to TIRF mode, always keeping the intensity of the laser power as low as possible (3% laser power). This procedure minimized photobleaching before image acquisition. Afterward, laser powers were set to 30% and image sequences (300–400 frames) were acquired with an exposure time of 30 ms, with an interval

between frames of 61.9 ms. The penetration depth of the evanescent field was ~110 nm. The microscope was equipped with an incubator and a temperature control unit (Tempcontrol 37-2 digital, PeCon). Experiments were performed at 20.5 ± 0.3 °C. Only cells with less than 0.45 receptor particle/μm^2 were analyzed.

3.5 MSD analysis

Single-molecule movies were processed using the NIH ImageJ software as reported in the previuosly described protocol (Sungkaworn et al., 2014), and then subjected to the computational analysis for particle detection and tracking following a recently described *u-track* algorithm implemented in Matlab (The Math Works) (Jaqaman et al., 2008). The diffusion speed of receptor particles was calculated on the basis of their mean square displacement (MSD) as explained in the work of Calebiro and colleagues (Calebiro et al., 2013).

3.6 Fluorescence Microscopy

For fluorescence microscopy analysis, CHO cells were plated on 13-mm coverslips at a density of $1,5 \times 10^5$ cells per well in p24 well plate and grown at 37°C for 18 h. Cells were then cotransfected with Lifeact-GFP, SNAP-tagged SSTR2 and FLNA 19-20/FLNA 17-18 using Lipofectamine 2000 as transfection reagent and following the instructions of the manufacturer. Receptors were labeled 24-48h after transfection and treated with saturating concentration (100nM) of BIM23120 up to 10 min to observe receptor clusters, and for 15, 30, and 60 min to monitor receptor internalization, at 37°C. Cells were then fixed with 4% paraformaldehyde for 10 min at room temperature, and washed several times in PBS (Thermofisher, Rockfor, IL). Coverslips were mounted on glass slides with ProLong Diamond Antifade mounting medium with 4',6-diamidino-2-phenylindole (DAPI) (Life Technologies, Carlsbad, CA) for fluorescence microscopy examination. Images acquisition

was performed using a Leica TCS SP2 laser scanning confocal microscope equipped with Ar 488nm and HeNe 543nm lasers (Leica Microsystem, Deerfield, IL). For internalization experiments, about 8-12 equatorial confocal sections from cell bodies were sequentially collected to ensure a scan thickness of ~ 500 nm and then images were processed with the NIH ImageJ software as subsequently described.

3.7 Immunofluorescence

CHO cells, transfected and treated as above described, were also used for immunofluorescence experiments. After fixation, cells were permeabilized with 0.3% Triton X-100 in PBS for 5 min and incubated with 10% FBS in PBS for 30 min to block unspecific sites. Cells were then incubated with a 1:250 dilution of anti AP-2 antibody (Thermofisher, Rockfor, IL) for 2 h at room temperature, washed 3 times with 0.05% Tween 20 in PBS and stained with Alexa Fluor 488 conjugated secondary antibody (Thermofisher, Rockfor, IL) for 1 h at room temperature. Both primary and secondary antibodies were diluted in an antibody dilution buffer containing 1% BSA, 0.3% Triton X-100 in PBS. After extensive washing, coverslips were mounted on glass slides and observed at the laser scanning confocal microscope for the analysis of SSTR2 - AP-2 colocalization.

3.8 Quantification of SSTR2 Internalization by Confocal Imaging

SSTR2 internalization was first evaluated by confocal microscopy. This imaging approach allows to analyze the amount of internalized receptor after agonist stimulation in single cells. The fluorescence density mean (F) in two distinct regions corresponding to the plasma membrane and to the whole intracellular area were densitometrically determined in each cell. Mean membrane to

intracellular fluorescence ratio (f_R) was then calculated as previously reported (Peverelli et al., 2008) according to the following equation:

f_R = [F(membrane) - F(background)] / [F(total) - F(background)].

The NIH ImageJ program was used to analyze at least 30 cells for each group from three independent transfections, and the mean value ± SD expressed as % of basal was used for the graph.

3.9 Quantitative Analysis of SSTR2 Internalization by Biotinylation Assay

Cell surface-proteins biotinylation assay was used to biochemically determine the receptor internalization rate. CHO cells transiently expressing wild type-SSTR2 were washed three times with ice-cold PBS, followed by a 30 min incubation with 500 µg/ml cleavable EZ-Link sulfo-NHS-SS-biotin (Thermofisher, Rockfor, IL) at 4 °C. Unreacted biotin was blocked and removed by three washes with cold Tris-buffered saline-10mM glycine. Biotinylated cells were incubated in prewarmed medium with or without 100 nM BIM23120 at 37 °C for 30 min, and then chilled on ice to stop SSTR2 endocytosis. Glutathione (Sigma-Aldrich, St. Louis, MO) was used to release the biotin label from proteins at the cell surface: cells were washed twice with cold glutathione strip buffer (50 mM glutathione, 75 mM NaCl, 75 mM NaOH, 10% FBS in H_2O), at 4 °C for 20 min. Excess of glutathione was then quenched by 30 min iodoacetamide (Sigma-Aldrich, St. Louis, MO) incubation at 4 °C. 50 mM Iodoacetamide was dissolved in a proper buffer containing 1% BSA, in PBS, pH 7.4. Cells were lysed with 100 µl lysis buffer and 60 µg of total cellular protein was incubated with 1 µg of SSTR2 (yI-17) antibody (Santa Cruz Biotechnology, Santa Cruz, CA) over night at 4 °C on a rotating device, for immunoprecipitation. The resuspended volume of protein A/G Plus-Agarose (20 µl) was then added, and tubes were incubated for 3 h at 4 °C in rotation. After 5 washes with ice-cold PBS, the pellet was resuspended in 45 µl of Blue loading buffer for immunoblotting. Eluted proteins were resolved by SDS-PAGE under nonreducing conditions. To detect biotinylated proteins, 1:500 dilution of anti-biotin, horseradish peroxidase-linked antibody

was used (Cell Signaling Technology, Danvers, MA). The presence of equal amounts of receptor in the immunoprecipitates was confirmed by stripping and reprobing with anti-SSTR2 antibody (1:200) and antimouse secondary antibody covalently coupled to horseradish peroxidase (1:2000). The resulting bands were analyzed with the NIH ImageJ software. Experiments were repeated in triplicate.

3.10 Statistical Analysis

Data were analyzed by unpaired Student *t* test and, where indicated, with Mann-Whitney test (Prism 5; GraphPad Software, San Diego, CA). The results are expressed as the mean ± SD or SEM and $P < 0.05$ was accepted as statistically significant.

4. RESULTS

4.1 Single molecule visualization of SSTR2 and FLNA

To directly observe SSTR2 and FLNA particles at the cell surface of living cells, we followed the procedure developed by Calebiro and collegues (Calebiro, et al., 2013). The functional activity of the SNAP-tagged receptor was confirmed by examining its ability to inhibit adenyl cyclase and reduce intracellular levels of cAMP (Fig. 1), whilst CLIP-tagged FLNA was validated for correct stress fibers organization and ability to colocalize with actin (Fig. 2A and B).

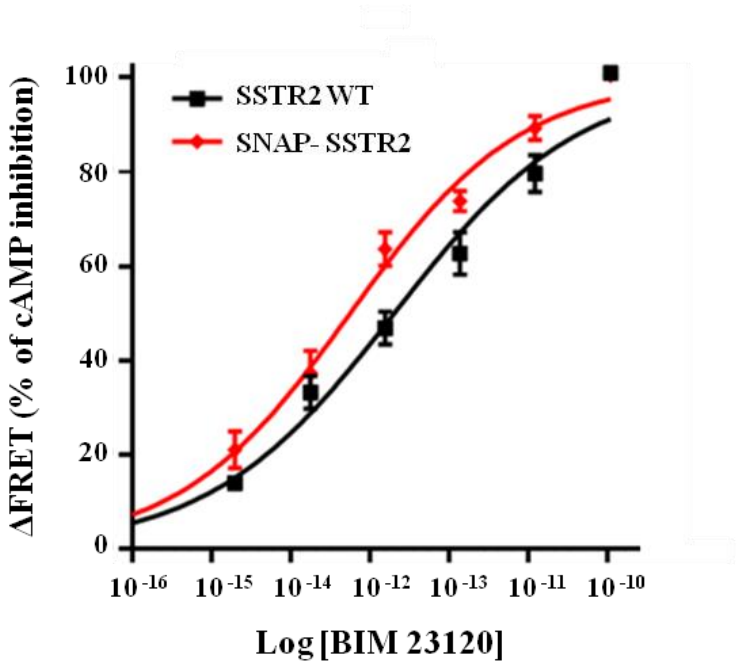

Figure 1. Functional characterization of SNAP-tagged SSTR2 construct. HEK293AD cells were transfected with SNAP-tagged SSTR2 or wild-type receptor together with Epac1-camps. Cells were incubated with increasing concentration of SSTR2 selective ligand BIM23120 and FRET measurements were performed to evaluate receptor ability of inhibiting the cAMP-production forskolin-triggered. SNAP-tagged SSTR2 construct is functional, as shown by cAMP concentration-response dependencies, comparable to those observed in wild-type SSTR2 transfected cells. Data are means ± SEM of 10 cells from three different experiments.

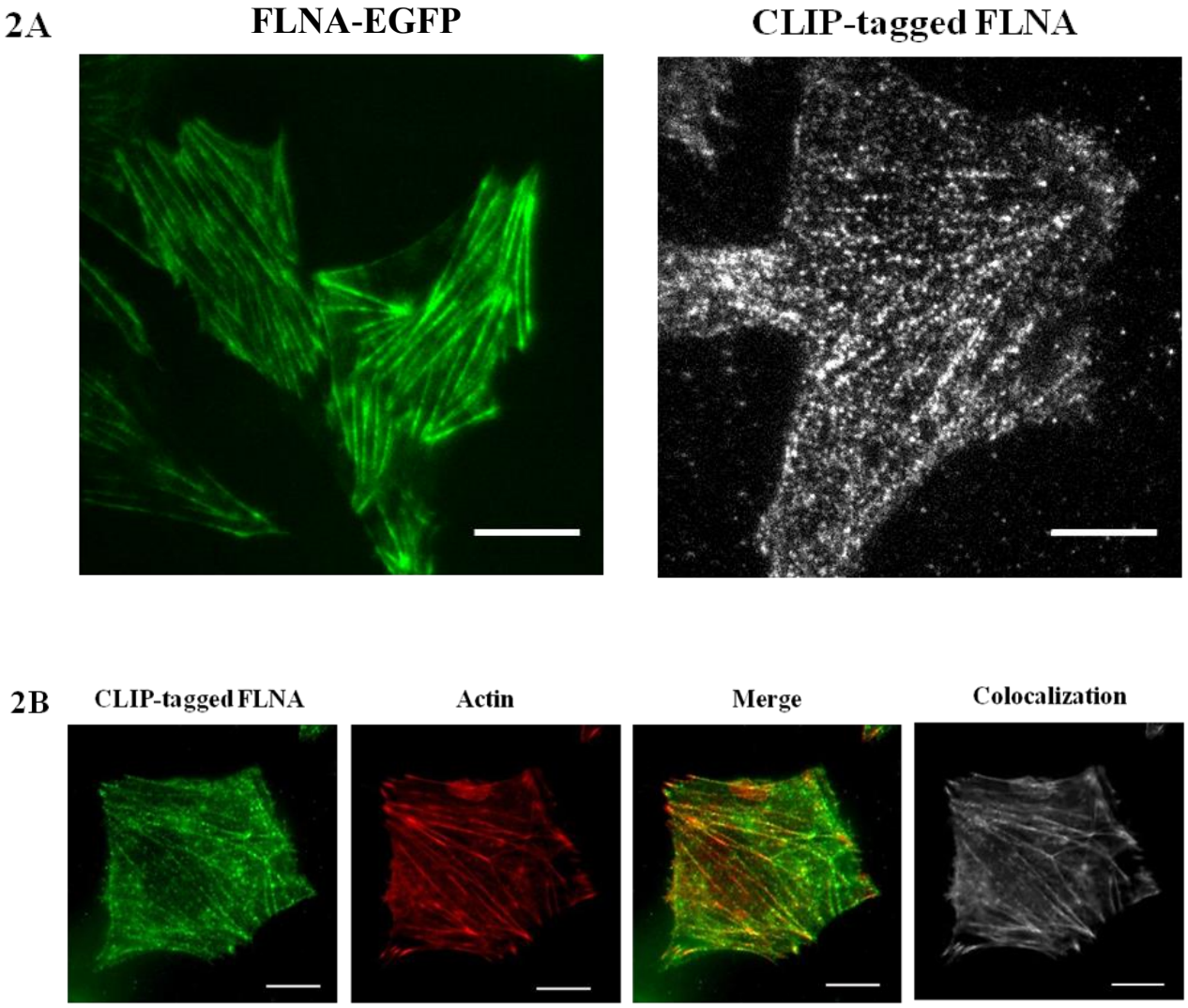

Figure 2. Validation of CLIP-tagged FLNA construct. (A) TIRF images of CHO cells transfected with FLNA-EGFP and CLIP-tagged FLNA, respectively. At the plasma membrane, CLIP-tagged FLNA construct displays the correct cell organization in stress fibers, similar to FLNA-EGFP. (B) TIRF images of CHO cell cotransfected with CLIP-tagged FLNA (green) and Lifeact-GFP (red). The colocalization between CLIP-tagged FLNA and actin filaments was analyzed by NIH ImageJ and is shown in white, confirming the actin-binding property of the CLIP-tagged FLNA construct. Scale bars, 10µm.

SNAP-tagged SSTR2 and CLIP-tagged FLNA were visualized in real time at the cell surface of CHO cells by TIRF microscopy (Fig. 3A, D). SSTR2 and FLNA particles detection (Fig. 3B, E) and tracking (Fig. 3C, F) was performed with the algorithm developed by Jaqaman and coworkers (Jaqaman K et al., 2008).

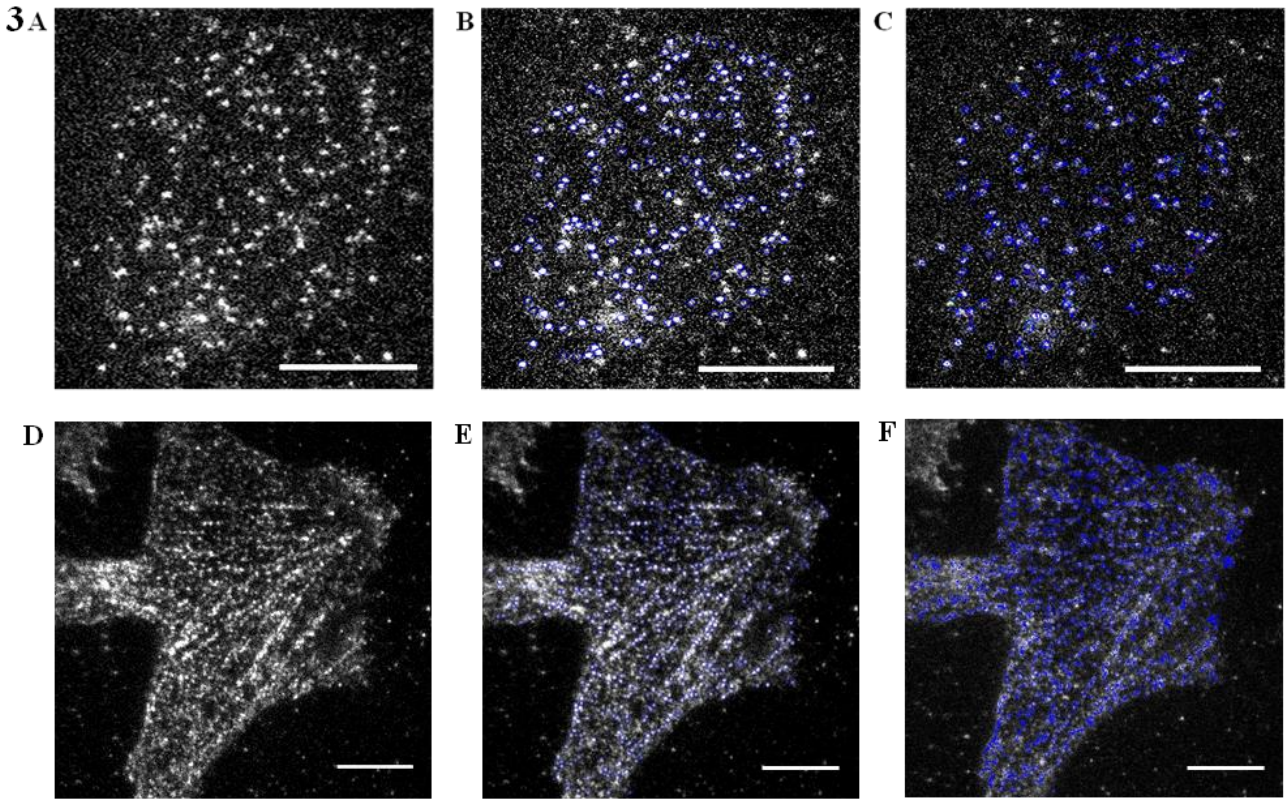

Figure 3. Single molecule visualization and tracking of individual SSTR2 and FLNA particles at the plasma membrane of living cells. CHO cells transfected with SNAP-tagged SSTR2 (A) or CLIP-tagged FLNA (D), labeled with Alexa647-BG and TMR-star dyes, respectively, and imaged by TIRF microscope. (B and E) Results of particle detection from images in A and D, respectively. (C and F) Representative images of particles tracking from detected particles in B and E, respectively; the current position (blue circle) and trajectory (blue spline) of each molecules are indicated. Scale bars, 10µm.

4.2 SSTR2 slow down after agonist stimulation

We evaluated the lateral mobility of functional SNAP-tagged SSTR2 particles at the plasma membrane in transfected CHO cells. Briefly, the individual SSTR2 particle coordinates over time were used to calculate their mean square displacement (MSD) and diffusion coefficient. Results from this analysis showed that under basal condition most receptors were freely diffusing at the cell surface. Interestingly, 5-10 min exposure to 100nM of the selective SSTR2 agonist BIM23120 slightly reduced SSTR2 diffusion speed (mean diffusion coefficient from 0,125$\mu m^{2*}s^{-1}$ to 0,110$\mu m^{2*}s^{-1}$), but caused a statistically significant enrichment in the receptor fraction characterized

by a limited mobility (particles with diffusion coefficient ≤ 0.05µm^{2*}s^{-1} = 28,1% in stimulated cells *vs* 14,4% in control cells, P < 0.05) (Fig. 4).

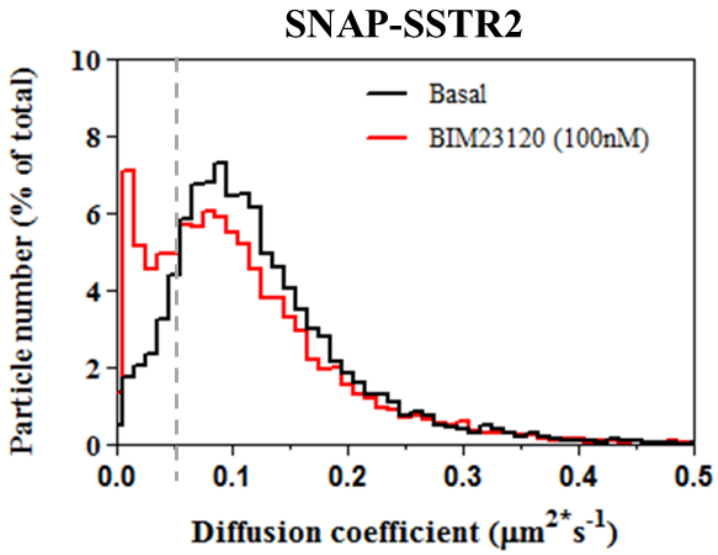

Figure 4. Effect of the SSTR2 selective agonist on receptor lateral mobility. CHO cells were transfected with SNAP-tagged SSTR2, labeled with 1 µM Alexa647-BG and stimulated or not with 100nM of BIM23120 for 5-10 min before image acquisition with TIRF microscope. The trajectories of individual SSTR2 particles were used to generate the distributions of their diffusion coefficient of treated cells (red line) compared with nonstimulated cells (black line). 100nM BIM23120 incubation slightly reduces SSTR2 mobility, but significantly increases the fraction of particles with diffusion coefficient values ≤ 0.05µm^{2*}s^{-1}. For particles with diffusion coefficient values in the range 0.00µm^{2*}s^{-1} - 0.05µm^{2*}s^{-1} the difference are statistically significant by Mann-Whitney test (P < 0.05).

To test a possible involvement of FLNA in mediating the agonist effect on the SSTR2 motion at the plasma membrane, we calculated the distribution of SSTR2 diffusion coefficients in CHO cells transiently overexpressing SSTR2 and FLNA 19-20, the FLNA fragment that plays a dominant negative effect for the binding of SSTR2 to the endogenous FLNA. FLNA 17-18 was used as a control peptide. It has to be taken into account that CHO cells endogenously express FLNA (Najib et al., 2012) and that the FLNA residues involved in SSTR2 binding are conserved between human and hamster. The incubation in the presence of 100nM BIM23120 resulted in a reduced receptor speed in respect to the resting condition, in both FLNA 17-18 transfected cells (mean diffusion coefficients from 0,123µm^{2*}s^{-1} to 0,101µm^{2*}s^{-1}) and FLNA 19-20 expressing cells (mean diffusion coefficients from 0,123µm^{2*}s^{-1} to 0,110µm^{2*}s^{-1}). However, no significant differences in SSTR2

lateral mobility were found in the absence of FLNA-SSTR2 interaction with respect to both basal and stimulated FLNA 17-18 expressing cells (Fig. 5).

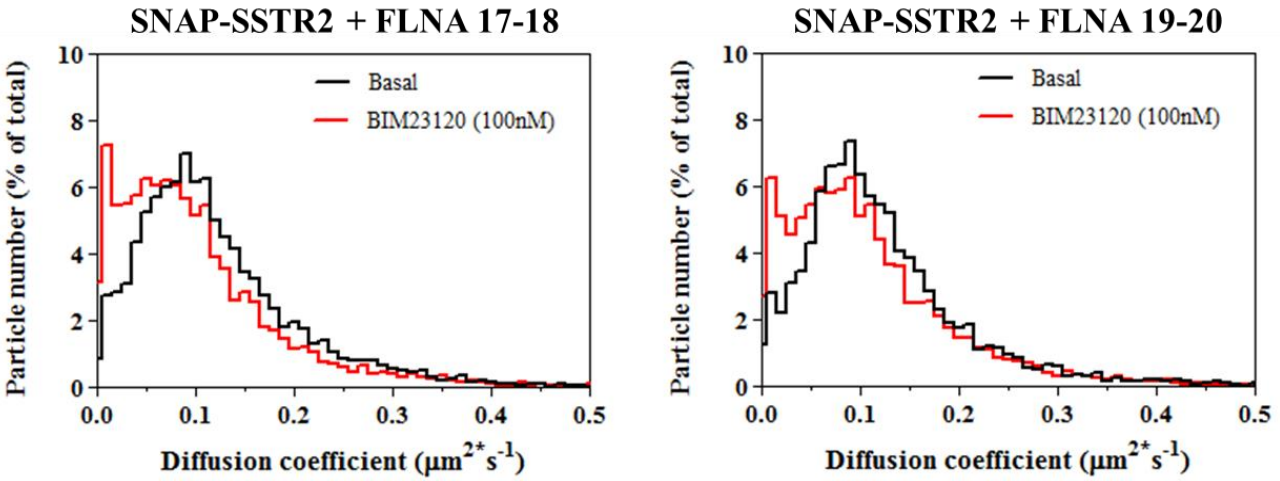

Figure 5. Testing an involvement of FLNA in regulating SSTR2 motion. CHO cells cotransfected with SNAP-tagged SSTR2 and FLNA 17-18 or FLNA 19-20 constructs, labeled with 1µM Alexa647-BG and treated or not with 100nM of BIM23120 for 5-10 min before image acquisition at TIRF microscope. Statistical analysis of the distributions of SSTR2 diffusion coefficients were performed with one-way ANOVA followed by Bonferroni's multiple comparison test and did not show any significant differences between FLNA 19-20 expressing cells compared with both control unstimulated and stimulated cells.

Similar results were obtained in human melanoma cell lines A7 (FLNA-expressing) and M2 (FLNA-lacking). It has to be mentioned that under basal condition SSTR2 were slightly more mobile in M2 cells compared to A7 cells (mean diffusion coefficient = 0,148$\mu m^{2*}s^{-1}$ *vs* 0,119$\mu m^{2*}s^{-1}$, in M2 *vs* A7 cell lines, respectively). Nevertheless, upon 100nM BIM23120 treatment, SSTR2 slow down in both cell lines, meaning that the complete lack of FLNA does not affect the action of SSTR2 agonist on receptor speed (Fig. 6).

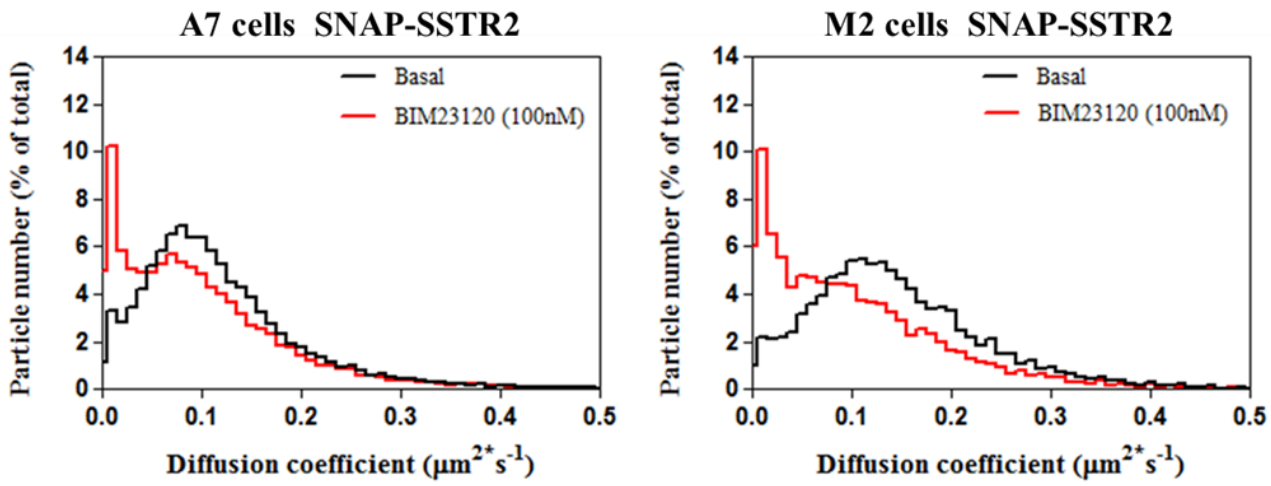

Figure 6. Evaluation of SSTR2 lateral mobility in A7 and M2 cell lines. A7 (FLNA-expressing) and M2 (FLNA-lacking) cell lines were transiently transfected with SNAP-tagged SSTR2 and labeled with 1μM Alexa647-BG dye. Image acquisitions were performed with TIRF microscope before and after 5-10 min of 100nM BIM23120 incubation. Upon stimulation, SSTR2 mean diffusion coefficient shifts from 0.119μm^{2*}s^{-1} to 0.101 μm^{2*}s^{-1} and from 0.148 μm^{2*}s^{-1} to 0.105μm^{2*}s^{-1}, in A7 and M2 cells respectively. There are no significant differences in SSTR2 lateral mobility in A7 cells compared to both treated and untreated M2 cells.

4.3 SSTR2 and FLNA undergo transient interactions which are increased by agonist stimulation and occur prevalently at actin fibers

We then investigated the dynamic behaviour of SSTR2-FLNA interactions in living CHO cells. We overexpressed the full-length FLNA-EGFP in order to visualize FLNA arrangement in fibers, and expressed SSTR2 at single molecule level to be able to follow the movement of single receptors along FLNA structures. Extremely dynamic and transient interactions between SSTR2 and FLNA fibers were observed and recorded under resting condition, whereas after 100nM BIM23120 treatment, SSTR2 was found to statically interact with FLNA structures, revealing a stronger affinity of binding between FLNA and ligand-activated receptors (Fig. 7).

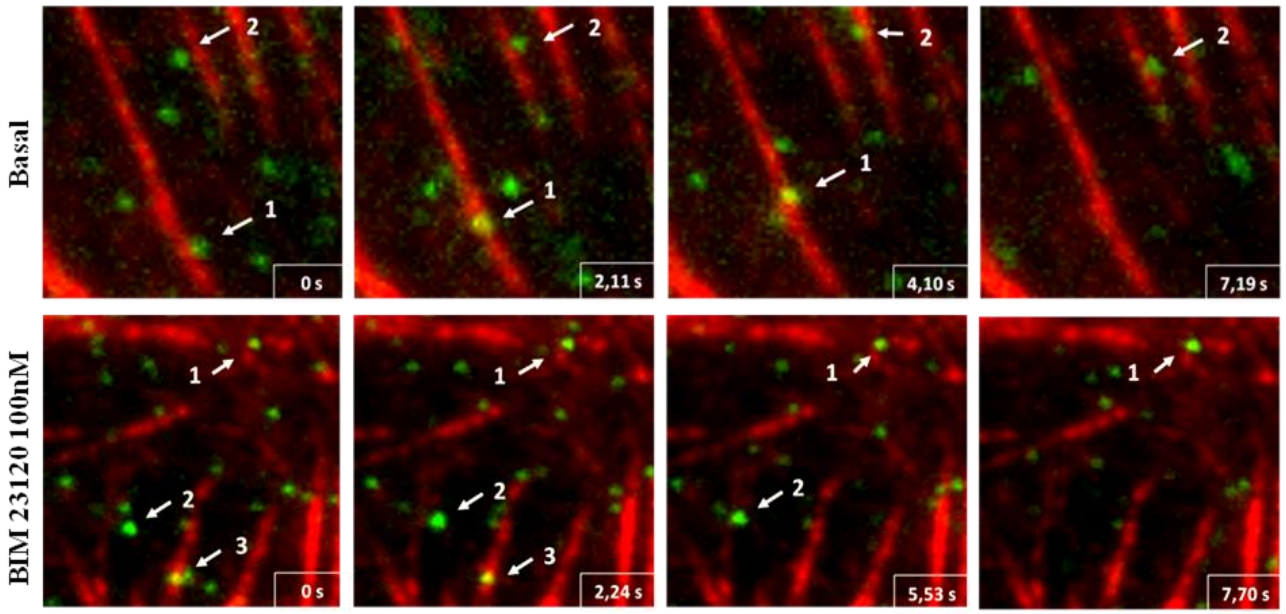

Figure 7. Dynamic visualization of SSTR2-FLNA interactions by TIRF-M. FLNA-EGFP (red) fibers and single molecules of SNAP-tagged SSTR2 (green) labelled with 1μM Alexa647-BG dye are expressed at the cell surface of cotransfected CHO cells. Representative frames of image sequences acquired by TIRF-M are here reported to characterize SSTR2-FLNA interactions occurred in real time, in both untreated and treated cells. The upper panel represents an example of dynamic interactions occurring between SSTR2-FLNA under resting condition: the arrows indicate two SSTR2 particles which transiently "touch" different side of the same FLNA filament (1) or get in contact with distinct FLNA fibers (2), respectively. The lower panel shows an example of static SSTR2-FLNA interactions resulted from 10 min stimulation with 100nM BIM23120: the arrows indicated agonist-activated receptors characterized by an absent or very limited mobility on FLNA fibers.

Next, we investigated the role of the cortical actin cytoskeleton in organizing SSTR2-FLNA complexes at the plasma membrane. To this aim we cotransfected CHO cells with single molecule expression levels of both CLIP-tagged FLNA and SNAP-tagged SSTR2, while Lifeact-GFP was overexpressed to allow the visualization of F-actin. Very temporary and short FLNA-SSTR2 interactions along actin filaments were observed under basal condition (Fig. 8), whilst in 100nM BIM23120 stimulated cells, static and long-lasting interactions between SSTR2 and FLNA particles were found to occur prevalently at actin fibers, suggesting an active role of the cortical actin network in spatially and temporally coordinating such SSTR2-FLNA complexes (Fig. 9).

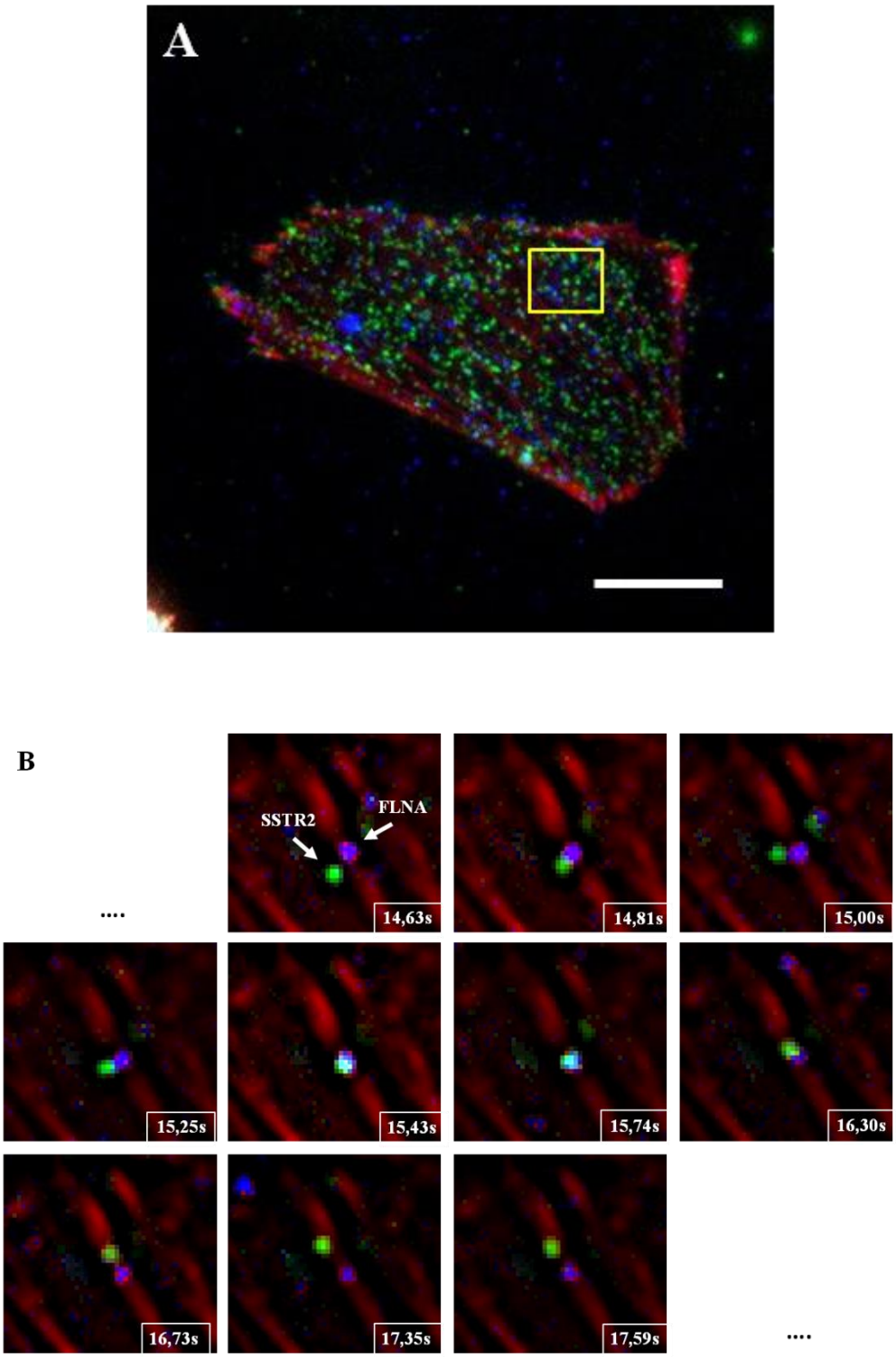

Figure 8. Single-molecule visualization of SSTR2-FLNA complexes interaction with actin cytoskeleton under resting conditions. (A) First frame of a representative TIRF-M image sequence acquired in living CHO cell expressing single-molecule levels of SNAP-tagged SSTR2 (green) and CLIP-tagged FLNA (blue), labeled with Alexa647-BG and TMR-STAR dyes, respectively and overexpressing Lifeact-GFP (red). Scale bar 10μM. (B) Higher magnification of the detail of the image sequence in A. Example of two distinct particles of SSTR2 and FLNA showing a dynamic and transient colocalization along an actin filament. A merging event (white) is quickly followed after some frames by a splitting event.

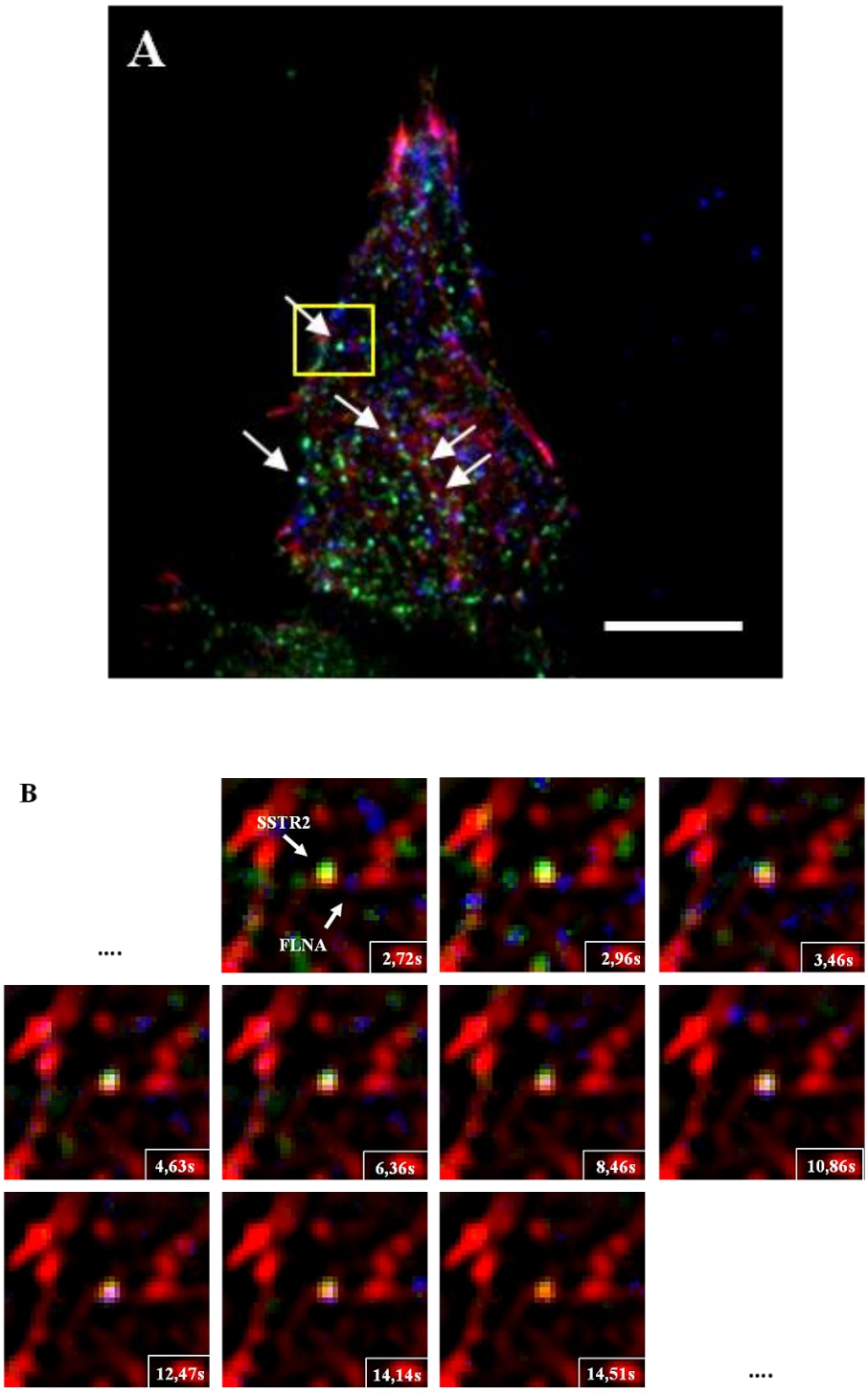

Figure 9. Single-molecule visualization of SSTR2-FLNA complexes interaction with actin cytoskeleton after receptor stimulation. (A) First frame of a representative TIRF-M image sequence acquired in living CHO cell expressing single-molecule levels of SNAP-tagged SSTR2 (green) and CLIP-tagged FLNA (blue), labeled with Alexa647-BG and TMR-STAR dyes, respectively and overexpressing Lifeact-GFP (red). The acquisition was performed after 10 min of receptor stimulation with 100nM BIM23120 and the picture shows several whitish spots (arrows) indicating SSTR2-FLNA particles colocalizing with actin fibers. Scale bar 10μM. (B) Higher magnification of the detail of the image sequence in A. Example of two distinct particles of SSTR2 and FLNA forming a stable and long-lasting complex localized on actin cytoskeleton. A merging event (white) lasts for several seconds until FLNA bleaching (last frame shown).

4.4 Disrupting SSTR2-FLNA interaction does not affect SSTR2 clustering formation but SSTR2 anchorage to actin cytoskeleton and organization in pits

To characterize more in detail the role of the actin cytoskeleton in organizing SSTR2 distribution at the cell surface, we performed confocal imaging experiments in CHO cells transfected with SNAP-tagged SSTR2 and Lifeact-GFP. Moreover, we overexpressed FLNA fragments to test the impact of the disrupted SSTR2-FLNA interaction on SSTR2 anchorage to actin structures. In absence of stimulation, SSTR2 resulted widely distributed at the plasma membrane in both control cells (cells cotransfected with Lifeact-GFP and FLNA 17-18, and cells expressing Lifeact-GFP, only) and in FLNA 19-20 expressing cells. After 10 min of SSTR2 agonist exposure, it was possible to appreciate a pattern of receptor clusters in all the tested conditions. Interestingly, the loss of FLNA-SSTR2 binding, achieved by overexpressing FLNA 19-20, did not affect SSTR2 clusters formation but rather impaired SSTR2 clusters alignment along actin fibers, which was preserved in stimulated control cells (Fig. 10). In fact, in the presence of the FLNA dominant negative mutant 19-20 most of the receptor clusters were spatially off-centered from the F-actin. These findings highlighted the important role of FLNA as a physical link between SSTR2 complexes and the cortical actin cytoskeleton, and suggested a possible involvement of FLNA in the regulation of SSTR2 early endocytotic events.

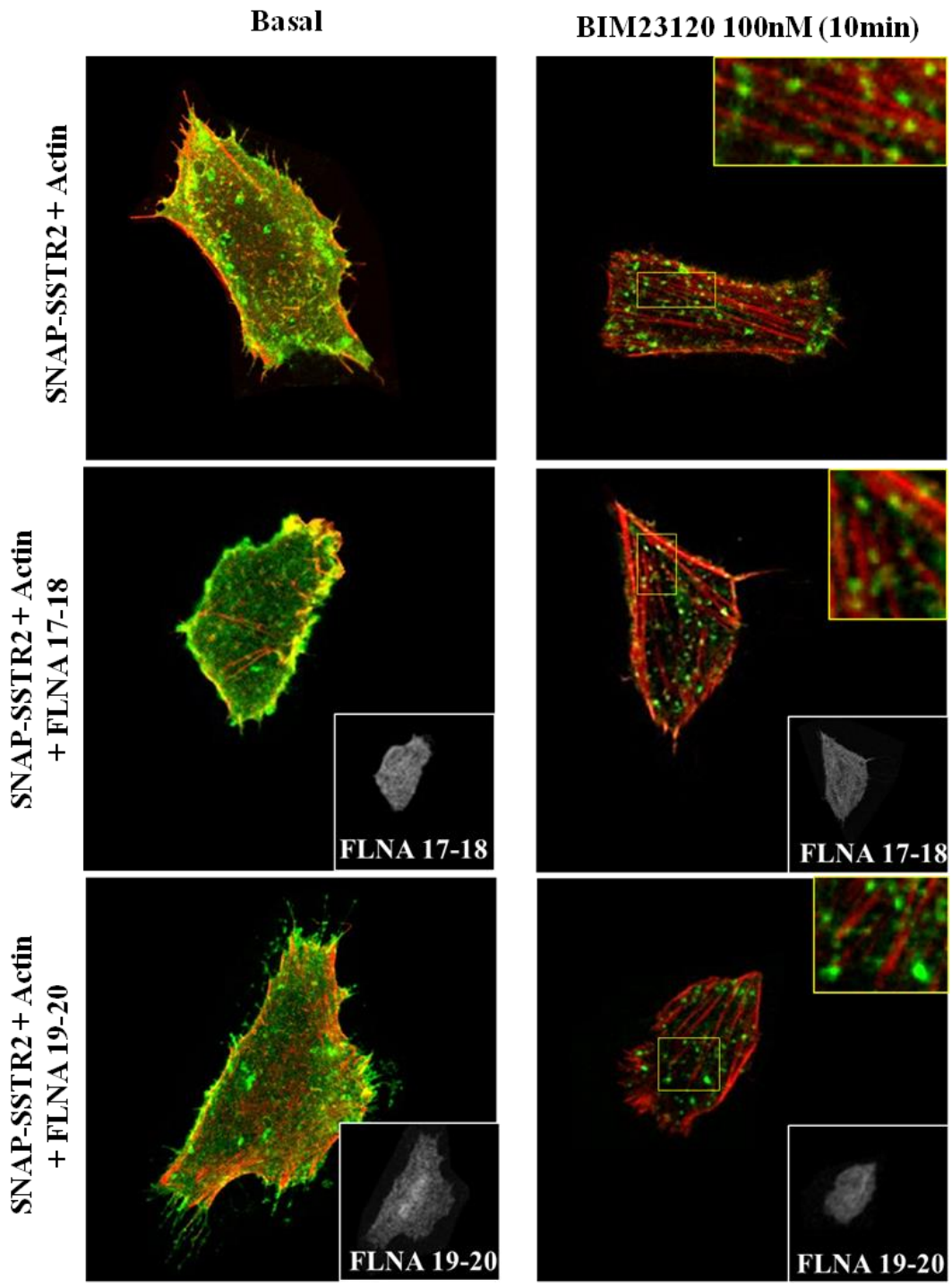

Figure 10. FLNA-SSTR2 binding preserves receptor clusters arrangement along actin filaments. CHO cells were transiently cotransfected with Lifeact-GFP (red), SNAP-tagged SSTR2 (green) and where indicated, FLNA truncated mutants FLNA 19-20/17-18 (white, lower inset). After labeling, cells were incubated in presence or absence of 100nM BIM23120 for 10 min at 37 °C, then fixed in PFA 4% and mounted on coverslips for confocal microscopy analysis. The figures are representative sections of the plasma membrane and show the overall SSTR2 distribution and localization in respect to the actin cortical cytoskeleton. (Left panel) Under basal condition, SSTR2 results widely spread at cell surface in control cells and FLNA 19-20 expressing cells. (Right panel) After BIM23120 incubation, SSTR2 clusters occurrence is visible in all the tested conditions. (Upper inset) Higher magnification of SSTR2 clusters localization along actin structures, showing that FLNA-SSTR2 binding is required to spatially anchor SSTR2 clusters to the cortical cytoskeleton, as observed in FLNA 17-18 transfected cells and cells expressing Lifeact-GFP only, but in FLNA 19-20 expressing cells.

To test this hypothesis, we first better defined the nature of the observed agonist-induced SSTR2 clusters, by immunofluorescence experiments. CHO cells, previously transfected with SNAP-tagged SSTR2 and FLNA truncated mutants, were immunostained for the adapting protein-2 (AP-2), a well-recognized clathrin-mediated endocytosis marker, to investigate the presence of SSTR2 clusters in clathrin-coated pits. As expected, after 5-10 min of 100nM BIM23120 exposure most of SSTR2 clusters colocalized with associated AP2 pits in FLNA 17-18 expressing cells. This degree of colocalization strongly decreased in FLNA 19-20 transfected cells, in the same condition of stimulation, thus suggesting a crucial scaffold role of FLNA in organizing the component of the endocytotic machinery (Fig. 11).

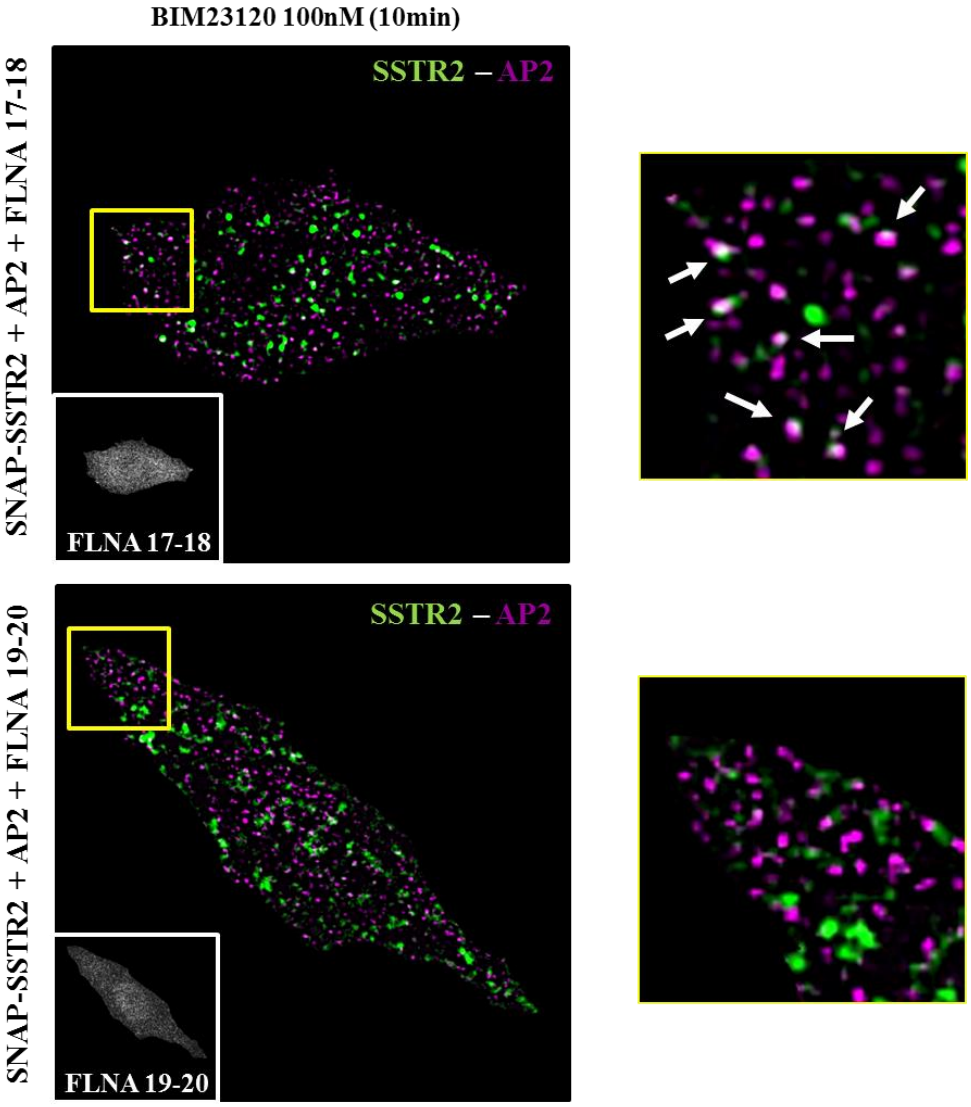

Figure 11. CHO cells were transiently cotransfected with SNAP-tagged SSTR2 (green) and FLNA truncated fragments FLNA 17-18/19-20 (white, lower inset). After receptor labeling, cells were treated with 100nM BIM23120 for 10 min at 37°C, then fixed in PFA 4% and immunostained for AP-2 (magenta) before mounting on coverslips. The figure shows representative confocal sections of the plasma membranes. Arrows in the magnification indicate colocalization events (white) between SSTR2 cluster and AP-2 defined pits which are present in control FLNA 17-18 expressing cells, only.

4.5 Interfering with SSTR2-FLNA interaction impairs SSTR2 internalization

Giving our observations of FLNA regulating the SSTR2 early endocytosis steps, we attempted to evaluate the impact of the abolished FLNA-SSTR2 interaction on the overall SSTR2 internalization process after agonist stimulation. Subcellular distribution of SSTR2 was analyzed by confocal microscopy in CHO cells transiently cotransfected with SSTR2 and FLNA fragments, incubated with or without 100nM BIM23120 for 15, 30 and 60 min as shown in figure 12. Before receptor stimulation SSTR2 was exclusively confined to the plasma membrane in both FLNA mutants expressing cells. The time course stimulation experiments showed a robust receptor internalization in control cells, already appreciable after 15 min of receptor activation, whilst it resulted strongly impaired in the absence of FLNA-SSTR2 coupling.

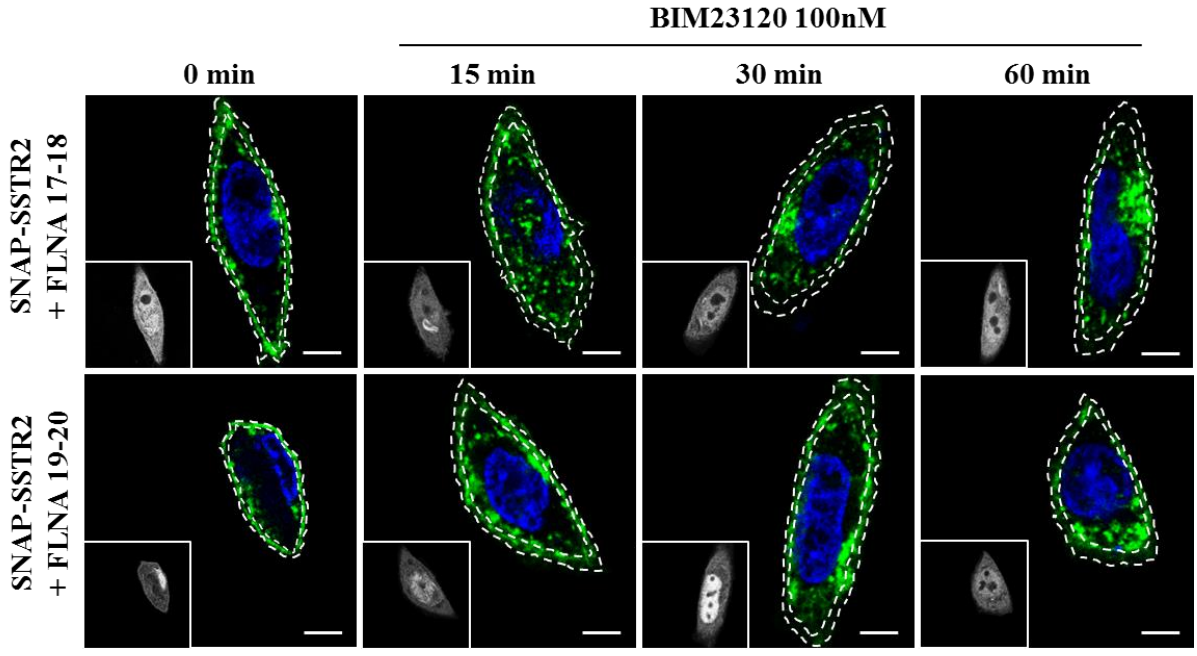

Figure 12. Impact of disrupted FLNA-SSTR2 interaction on agonist-mediated SSTR2 internalization. CHO cells transiently overexpressing SNAP-tagged SSTR2 (green) and FLNA truncated mutants (white inset) FLNA 17-18 and

FLNA 19-20, upper and lower panel, respectively, were stained with 1µM Alexa647-BG dye and incubated with 100nM BIM23120 for 0, 15, 30, and 60 min. DAPI was used to stain the nucleus. Fixed cells were analyzed by confocal microscopy. The figures show intracellular sections representative of receptor translocation from the plasma membrane to the interior compartment. In FLNA 17-18 expressing cells the receptor internalization rate increases through the time window considered, whereas it results significantly reduced in presence of FLNA 19-20, as demonstrated by the abundant presence of cell surface SSTR2 staining after 30 - 60 min of receptor stimulation.

The quantitative analysis, performed by calculating the membrane to intracellular SSTR2 fluorescence ratio (f_R), reported that the lack of FLNA-SSTR2 interaction significantly reduced SSTR2 internalization rate at all the tested time points, as reported in the graph and table below (Fig. 13).

	% SSTR2 internalization	
Time (min)	FLNA 17-18 expressing cells	FLNA 19-20 expressing cells
0'	30,9 ± 7,2	29,9 ± 5,7
15'	54,8 ± 10,3	41,4 ± 2,8
30'	68,7 ± 3,6	45,3 ± 1,4
60'	71,4 ± 3,1	53,0 ± 2,7

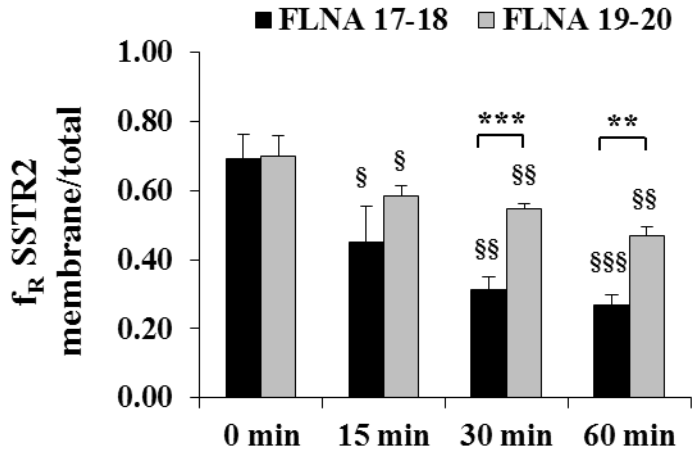

Figure 13. Quantitative analysis of SSTR2 internalization rate. A) The quantitative analysis of SSTR2 internalization from confocal images was performed by calculating the fR with NIH ImageJ program. For each group, at least 30 cells from three independent transfections were analyzed. B) Histograms showing the results of quantitative analysis of SSTR2 internalization from confocal images. For each group, at least 15 cells from three independent transfections were analyzed by calculating the fR with NIH ImageJ program. Mean ± SD values were used for the graph. **, $P < 0.01$, *** $P < 0.001$ vs FLNA 17-18 expressing cells; §, $P < 0.05$, §§, $P < 0.01$ vs respective basal.

To confirm this result we performed a biochemical assay of surface biotinylated proteins. Accordingly, we demonstrated that SSTR2 internalization occurring in cells transfected with FLNA 17-18 was strongly reduced in cells expressing FLNA 19-20 (39,1% ± 11,6% internalization *vs* 9,0% ± 3,4% in cells expressing FLNA 17-18 *vs* FLNA 19-20, respectively, $P < 0.05$ after 30 min of 100nM BIM23120 incubation (Fig. 14).

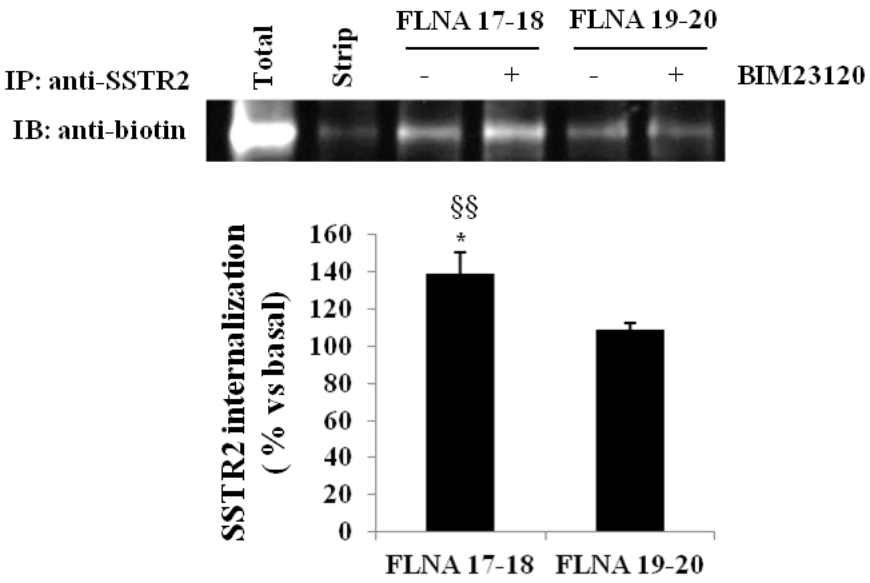

Figure 14. SSTR2 internalization determination by biotinylation assay. A representative biotinylation experiment is shown. CHO cells transiently transfected with FLNA 17-18 or FLNA 19-20 and wild-type SSTR2 were treated or not with 100nM BIM23120 for 30 min. Surface receptors were then biotinylated and cells were lysed. SSTR2 immunoprecipitation was assessed by using an anti-SSTR2 antibody and immunoblotting was performed with an anti-biotin antibody as described in material & methods. SSTR2 internalization is expressed as a percentage relative to basal, normalized to the total amount of receptor. The densitometrical analysis was performed by NIH ImageJ software for three independent experiments and the mean value ± SD was used for the graph. *, $P < 0.05$ FLNA 17-18 vs FLNA 19-20 transfected cells; §§ = $p<0.01$ vs respective basal.

5. DISCUSSION

The present research investigated the dynamics of SSTR2-FLNA interactions at the plasma membrane level, revealing a crucial active role of the cytoskeleton protein FLNA in spatially and temporally coordinating SSTR2 internalization.

In an attempt to better understand the molecular determinants at the basis of the pharmacological resistance to SSA displayed by a subset of acromegalic patients, FLNA has been recently pointed out as a new modulator of the activity and stability of SSTR2 (Peverelli et al., 2014), which is the SSTR subtype mostly expressed at the surface of GH-secreting tumoral cells. However, compared with the large series of studies dealing with SSTR2 signaling, SSTR2 dynamics under resting conditions or after agonist activation are mostly unexplored *in vivo*, and to date, there are no evidence describing the behavior of SSTR2-FLNA interactions in living cells. Here, we used the single molecule live-cell imaging approach to visualize, in real time, the formation of FLNA-SSTR2 complexes at the cell surface and study the impact of FLNA-SSTR2 binding on receptor mobility. Moreover, we investigated the FLNA linking role between SSTR2 and the cortical actin cytoskeleton and its involvement in SSTR2 agonist induced-endocytosis.

Previous works demonstrated the efficiency of the strategy which combines single molecule TIRF-M, and the direct labeling of the protein of interest with small organic fluorophores through SNAP/CLIP-tags, to perform dynamic studies (Keppler et al., 2003; Kasai et al., 2011; Calebiro et al., 2013). SNAP-tagged SSTR2 and CLIP-tagged FLNA were considered valuable tools for our investigations. In fact, SNAP-tagged receptor displayed the correct cell distribution and maintained the ability to couple to the Gi/o signal transduction pathway, in terms of cAMP inhibition upon stimulation, as the wild type-receptor. CLIP-tagged FLNA showed the typical subcellular localization in stress fibers and colocalized with actin filaments, thus confirming that the insertion

of tags within the first hinge region of the FLNA monomer does not interfere with its actin binding properties (Planagumà et al., 2012).

First, the analysis of receptor mobility revealed that SSTR2 freely diffuses at the plasma membrane in living cells. Moreover, the percentage of the mobile fraction is very high (>86%) under resting condition. This finding was completely in agreement with the fluorescence recovery after photobleaching (FRAP) results obtained with murine SST2a, in living hippocampal neurons (Lelouvier et al., 2008). The dynamic properties of SSTR2 are modulated by the agonist stimulation, as demonstrated by a significant increase in the immobile receptor fraction compared to the basal state. These data seem to indicate that normally only a minor population of SSTR2 might be associated with cytoskeleton anchoring proteins, whereas such interactions more often occur when the receptor is activated. This observation is true for other GPCRs such as the β-adrenergic receptor (Hall et al., 1998), whilst it does not seem the case of $GABA_B$ receptor, whose limited mobility is accelerated by the effect of GABA, likely due to a diminished binding with the cortical actin filaments (Calebiro et al., 2013).

However, SSTR2 speed is not regulated by FLNA interaction. As shown by MSD analysis, the presence of the FLNA truncated mutant FLNA 19-20, which selectively prevents the endogenous FLNA binding to SSTR2, did not affect SSTR2 lateral diffusion in any condition. FLNA repeats 19-20 are known to contain the SSTR2-binding region (Najib et al., 2012) and the overexpression of this FLNA fragment was recently successfully used to understand the impact of the abolished SSTR2-FLNA complex formation on receptor signaling and downregulation in GH-secreting cells (Peverelli et al., 2014). To note that this dominant negative approach was validated by another study with the purpose to avoid D2R-FLNA interaction (Lin et al., 2002). We excluded the hypothesis of a possible role of FLNA in the regulation of SSTR2 mobility by performing single-molecule experiments in A7 and M2 cell lines. According to our observation, high-resolution particle tracking showed no differences in the total mobility of Cav1–GFP vesicles over a time scale of 60 seconds regardless of FLNA expression (Muriel et al., 2011). Nevertheless, the same TIRF-M

strategy was used to evaluate the diffusion of membrane associated vesicles, which resulted significantly decreased in cells with reduced FLNA (Sverdlov et al., 2009).

Next, we analyzed the nature of SSTR2-FLNA interactions in living CHO cells transfected with single-molecule levels of SSTR2 and overexpressing FLNA-EGFP. Interestingly, dynamic and transient SSTR2-FLNA interactions observed under basal condition became more stable and long-lasting upon 5-10 min of SSTR2 agonist exposure. Therefore, even though upon SSTR2 stimulation FLNA does not contribute to the enrichment of the immobile receptor fraction, it seems to act as scaffold platform where ligand-activated receptors preferentially stop, likely to initiate their signaling transduction, then followed by internalization. It is to be taken into account that these imaging data might be consistent with the immunoprecipitation results obtained by Najib and co-workers, which illustrated an increase of FLNA recruitment to SSTR2 and MOR, upon ligand treatment, in BON and SH-SY5Y cells, respectively (Najib et al., 2012).

Moreover, we demonstrated a key role of the cortical actin cytoskeleton in the compartimentalization of agonist-induced SSTR2-FLNA complexes. As recorded by our single molecule movie clips, long-lasting colocalizations between SSTR2 and FLNA single particles occurred along actin filaments at the cells surface of living CHO cells, under stimulation condition, only. The dynamics of these interactions may be ruled by the "membrane-skeleton fence model" previously proposed (Tsuji et al., 1988; Kusumi et al., 1993). This model describes a membrane-associated cytoskeleton meshwork, also called membrane skeleton, as a physical barrier to the free diffusion of transmembrane proteins, which in turn confines their motion into defined compartments of the plasma membrane. The finely regulated dissociation-association equilibrium of the cytoskeleton continuously modulates the dynamic properties of the membrane skeleton, so that the space between the membrane and the skeleton may vary over time, giving the membrane proteins the chance to cross the barrier and reach specific domains within the cells surface.

When overexpressed and stimulated for 5-10 min with the agonist, SSTR2 was observed to undergo cluster formation at the level of the plasma membrane, whereas it was widely distributed throughout

the cell surface in absence of stimuli. The receptor arrangement in clusters and their alignment along actin filaments were explored by confocal microscopy in presence of FLNA truncated mutants. Our observation showed that the disruption of SSTR2-FLNA interaction did not affect the SSTR2 organization in clusters. A similar finding has been reported for the chemokine (C-C motif) receptor 2B (CCR2B), where no difference in receptor clusterization was seen at the plasma surface of A7 and M2 cells, although a less reduction in the overall number of clusters upon ligand incubation was detected in FLNA depleted cells with respect to A7 cells, demonstrating the involvement of FLNA in regulating CCR2B endocytosis (Minsaas et al., 2010).

Interestingly, we detected a remarkably reduced colocalization between SSTR2 clusters and actin filaments in presence of FLNA 19-20 compared to controls, showing that SSTR2 clusters cannot properly associate with the actin cytoskeleton without binding to FLNA.

Furthermore, we demonstrated that like for other GPCRs and transmembrane proteins, FLNA interaction is required to initiate and sustain SSTR2 endocytosis (Lin et al., 2001; Cho et al., 2002; Onoprishvili et al., 2003; Seck et al., 2003; Zhang & Breitwieser, 2005; Minsaas et al., 2010; Muriel et al., 2011; Noam et al., 2014). SSTR2 endocytosis is known to be clathrin-coated pit mediated since it is inhibited by hypertonic sucrose, a common reagent used to block clathrin lattice formation (Koenig et al., 1998). Among the different proteins which cooperate to the formation of clathrin coated vesicles, the heterotetrameric adaptor complex AP-2 is one of the factor which identify nascent vesicles at the plasma membrane, since it disengages from sites of endocytosis seconds before intenalization (Rappaport et al., 2006). We performed AP-2 immunostaining to confirm that SSTR2 clusters were actually accumulated in nascent clathrin coated pits. We found a decrease in the colocalization rate between agonist-induced SSTR2 clusters and AP2-defined pits caused by the abolished SSTR2-FLNA interaction, strongly supporting a role for FLNA in mediating a cytoskeletal spatial orientation of coated pits. The actin cytoskeleton has been implicated in the maintenance of discrete sites of clathrin-coated pit assembling during receptor endocytosis. In addition, the observation that such pits tend to form repeatedly at defined regions

while excluding others has been attributable to the attachment of the pits to the membrane skeleton (Gaidarov et al., 1999; Bennet et al., 2001). Moreover, the actin network has been postulated to play both a structural role in clathrin-coated mediated endocytosis (CME), controlling the localization of endocytotic machinery on the plasma membrane, and a mechanical role, providing the force to drive invagination and translocation of the nascent vesicles into the cytoplasm (Qualmann et al., 2000; Qualmann & Kessels, 2002; Merrifield et al., 2002; Engqvist-Goldstein & Drubin, 2003). Here, we described FLNA as a potential molecular link between SSTR2 clusters/coated pits and actin. A similar clathrin/actin linker role has been previously characterized for other actin binding proteins such as the huntingtin interacting protein 1 related (Hip1R) (Bennet et al., 2001).

The imaging and biochemical studies presented in the present work clearly demonstrate a crucial role for FLNA not only in the regulation of the early endocytotic events, but also in the overall SSTR2 internalization process. CHO cells displayed an agonist-induced SSTR2 internalization kinetic comparable to the ones already described in the literature (Koenig et al., 1997; Liu et al., 2005; Liu et al., 2008; Cambiaghi et al., 2016), with about 70-80% of receptor completely localized in the intracellular compartment upon 30 min of agonist exposure, whereas it was strongly impaired when FLNA-SSTR2 association was prevented. The much slower internalization rate observed in FLNA-19-20 transfected cells might be due to an inefficient translocation of the nascent vesicles from the plasma membrane to the endosomes, a step which probably requires FLNA scaffold functions to properly orchestrate the endocytotic machinery without leaving some receptors at the cell surface. Indeed, a strong membrane staining of SSTR2 was visible at all the tested time points of stimulation in FLNA 19-20 expressing cells. Though, further experiments are required to examine the presence of possible alterations in the vesicles intracellular trafficking after the initial endocytosis, in cells lacking FLNA-SSTR2 interaction. However, it has to be mentioned that Najib and colleagues showed an accelerated SSTR2 internalization rate in A7 cells compared to M2 cells upon ligand treatment (Najib et al., 2012). The discrepancy between this data and our results might be due to cell-specific FLNA functions, and/or to the different approach used. In fact, the dominant

negative effect played by FLNA 19-20 in CHO cells selectively abrogates SSTR2-FLNA coupling without affecting the endogenous FLNA ability to cross-link and organize actin filaments into a dynamic cytoskeleton network, a property which is completely lost in M2 cells.

Altogether the results presented in this thesis let us to speculate that, by tethering SSTR2 to actin filaments, FLNA may facilitate the formation of ligand-inducible complexes with interacting proteins that are necessary for the efficient endocytosis of the receptor into clathrin-coated vesicles. In this regard, it is possible that FLNA may coordinate the interaction between SSTR2 and β-arrestins. It is well established that after the phosphorylation of Ser/Thr residues located at its C-tail, SSTR2 is able to recruit both β-arrestins, and together undergo internalization (Hipkin et al., 1997; Tulipano et al., 2004; Liu et al., 2005; Lehmann et al., 2014; Cambiaghi et al., 2016). Moreover, β-arrestins binding site to FLNA involves repeat 22 of the FLNA monomer (Kim et al., 2005; Scott et al., 2006). A recent research focused on CCR2B and performed in melanoma cell lines, showed that in absence of FLNA β-arrestin 2 still binds to the receptor, but a delay in the formation of clathrin coated pits and in the receptor internalization occurs. Also in this case, the fate of the stimulated receptor seems to be dependent on FLNA association with components of the endocytotic machinery (Minsaas et al., 2010). As regards SSTR2, additional studies are needed to investigate the presence and eventually the biological meaning of SSTR2-FLNA-β-arrestins complexes at the plasma membrane.

In conclusion, for the first time SSTR2-FLNA interactions were evaluated by means of a high spatio-temporal resolution technique, revealing the *in vivo* dynamics and the importance of this interaction for SSTR2 anchorage to the actin cortical cytoskeleton and internalization. Since a role for FLNA in the regulation of ligand-mediated SSTR2 signaling and downregulation has been already demonstrated in GH-secreting cells (Peverelli et al., 2014), it becomes relevant to continue elucidating the involvement of FLNA in the formation of compartmentalized domains at the plasma membrane, where SSTR2 are first assembled into functional units, and then subjected to endocytosis. Indeed, a deeper understanding of both these aspects may be useful to clarify the

molecular mechanisms by which the cells can modulate the amount of active receptors at their surface, thus determining a variable responsiveness to SSAs, with possible implications in the pharmacological resistance seen in the clinical management of acromegaly.

6. REFERENCES

Abe T, Ludecke DK. Recent primary transnasal surgical outcomes associated with intraoperative growth hormone measurement in acromegaly. *Clin Endocrinol (Oxf)* 1999; 50(1): 27-35

Asa SL, Scheithauer BW, Bilbao JM, Horvath E, Ryan N, Kovacs K, Randall RV, Laws ER, Jr Singer W, Linfoot JA, Thorner MO, Vale W. A case for hypothalamic acromegaly: a clinicopathological study of six patients with hypothalamic gangliocytomas producing growth hormone-releasing factor. *J Clin Endocrinol Metab* 1984; 58(5): 796-803

Ballarè E, Mantovani S, Bassetti M, Lania A, Spada A. Immunodetection of G proteins in human pituitary adenomas: evidence for a low expression of proteins of the Gi subfamily. *Eur J Endocrinol* 1997; 137(5): 482-9

Ballarè E, Persani L, Lania AG, Filopanti M, Giammona E, Corbetta S, Mantovani S, Arosio M, Beck-Peccoz P, Faglia G, Spada A. Mutation of somatostatin receptor type 5 in an acromegalic patient resistant to somatostatin analog treatment. *J Clin Endocrinol Metab* 2001; 86(8): 3809-14

Barlier A, Pellegrini-Bouiller I, Gunz G, Zamora AJ, Jaquet P, Enjalbert A. Impact of gsp oncogene on the expression of genes coding for Gsalpha, Pit-1, Gi2alpha, and somatostatin receptor 2 in human somatotroph adenomas: involvement in octreotide sensitivity. *J Clin Endocrinol Metab* 1999; 84(8): 2759-65

Bassetti M, Spada A, Arosio M, Vallar L, Brina M, Giannattasio G. Morphological studies on mixed growth hormone (GH)- and prolactin (PRL)-secreting human pituitary adenomas. Coexistence of GH and PRL in the same secretory granule. *J Clin Endocrinol Metab* 1986; 62(6): 1093-100

Batista DL, Zhang X, Gejman R, Ansell PJ, Zhou Y, Johnson SA, Swearingen B, Hedley-whyte ET, Stratakis CA, Klibanski A. The effects of SOM230 on cell proliferation and ACTH secretion in human corticotroph pituitary adenomas. *J Clin Endocrinol Metab* 2006; 91: 4482-8

Bauer W, Briner U, Doepfner W, Haller R, Huguenin R, Marbach P, Petcher TJ, Pless. SMS 201-995: a very potent and selective octapeptide analogue of somatostatin with prolonged action. *Life Sci* 1982; 31(11): 1133-40

Beal MF, Mazurek MF, Ellison DW, Swartz KJ, McGarvey U, Bird ED, Martin JB. Somatostatin and neuropeptide Y concentrations in pathologically graded cases of Huntington's disease. *Ann Neurol* 1988; 23: 562-569

Beekman JM, van der Poel CE, van der Linden JA, van den Berg DL, van den Berghe PV, van de Winkel JG, Leusen JH. Filamin A stabilizes Fc gamma RI surface expression and prevents its lysosomal routing. *J Immunol* 2008; 180(6): 3938-45

Bennett EM, Chen CY, Engqvist-Goldstein AE, Drubin DG, Brodsky FM. Clathrin hub expression dissociates the actin-binding protein Hip1R from coated pits and disrupts their alignment with the actin cytoskeleton. *Traffic* 2001; 2(11): 851-8

Ben-Shlomo A, Melmed S. Acromegaly. *Endocrinol Metab Clin North Am*. 2008; 37(1): 101-22

Ben-Sholmo A, Melmed S. Pituitary somatostatin receptor signaling. *Trends Endocrinol Metab* 2010; 21(3): 123-33

Ben-Shlomo A, Pichurin O, Khalafi R, Zhou C, Chesnokova V, Ren SG, Liu NA, Melmed S. Constitutive somatostatin receptor subtype 2 activity attenuates GH synthesis. *Endocrinology* 2013; 154: 2399–2409

Berryman DE, Palmer AJ, Gosney ES, Swaminathan S, Desantis D, Kopchick, JJ. Discovery and uses of pegvisomant: A growth hormone antagonist. *Endokrynologia Polska* 2007; 58(4): 322–9

Bertherat J, Bluet-Pajot MT, Epelbaum J. Neuroendocrine regulation of growth hormone. *Eur J Enodcrinol* 1995; 132: 12-24

Bocca L, Valenti S, Cuttica CM, Spaziante R, Giordano G, Giusti M. Nitric oxide biphasically modulates GH secretion in cultured cells of GH-secreting human pituitary adenomas. *Minerva Endocrinol* 2000; 25(3–4): 55–59

Bousquet C, Guillermet-Guibert J, Saint-Laurent N, Archer-Lahlou E, Lopez F, Fanjul M, Ferrand A, Fourmy D, Pichereaux C, Monsarrat B, Pradayrol L, Estève JP, Susini C. Direct binding of p85

to sst2 somatostatin receptor reveals a novel mechanism for inhibiting PI3K pathway. *EMBO J* 2006; 25(17): 3943-54

Brada M, Burchell L, Ashley S, Traish D. The incidence of cerebrovascular accidents in patients with pituitary adenoma. *Int J Radiat Oncol Biol Phys* 1999; 45: 693-8

Brazeau P, Vale W, Burgus R, Ling N, Nutcher M, Rivier J, Guillemin R. Hypothalamic polypeptide that inhibits the secretion of immunoreactive pituitary growth hormone. *Science* 1973; 179: 77–79

Bruns C, Weckbecker G, Raulf F, Kaupmann K, Schoeffter P, Hoyer D, Lübbert H. Molecular pharmacology of somatostatin-receptor subtypes. *Ann NY Acad Sci* 1994; 733: 138–146

Bruns C, Lewis I, Briner U, Meno-Tetang G, Weckbecker G. SOM230: a novel somatostatin peptidomimetic with broad somatotropin release inhibiting factor (SRIF) receptor binding and a unique antisecretory profile. *Eur J Endocrinol* 2002; 146(5): 707-16

Brzana J, Yedinak CG, Gultekin SH, Delashaw JB, Fleseriu M. Growth hormone granulation pattern and somatostatin receptor subtype 2A correlate with postoperative somatostatin receptor ligand response in acromegaly: a large single center experience. *Pituitary* 2013; 16(4): 490-8

Buscail L, Estève JP, Saint-Laurent N, Bertrand V, Reisine T, O'Carroll AM, Bell GI, Schally AV, Vaysse N, Susini C. Inhibition of cell proliferation by the somatostatin analogue RC-160 is mediated by somatostatin receptor subtypes SSTR2 and SSTR5 through different mechanisms. Proc *Natl Acad Sci USA* 1995; 92: 1580–1584

Calebiro D, Rieken F, Wagner J, Sungkaworn T, Zabel U, Borzi A, Cocucci E, Zürn A, Lohse MJ. Single-molecule analysis of fluorescently labeled G-protein-coupled receptors reveals complexes with distinct dynamics and organization. *Proc Natl Acad Sci U S A* 2013; 110(2): 743-8

Cambiaghi V, Vitali E, Morone D, Peverelli E, Spada A, Mantovani G, Lania AG. Identification of human somatostatin receptor 2 domains involved in internalization and signaling in QGP-1 pancreatic neuroendocrine tumor cell line. Endocrine 2016; Epub ahead of print

Casarini AP, Pinto EM, Jallad RS, Giorgi RR, Giannella-Neto D, Bronstein MD. Dissociation between tumor shrinkage and hormonal response during somatostatin analog treatment in an acromegalic patient: preferential expression of somatostatin receptor subtype 3. *J Endocrinol Invest* 2006; 29: 826–830

Castillo V, Theodoropoulou M, Stalla J, Gallelli MF, Cabrera-Blatter MF, Haedo MR, Labeur M, Schmid HA, Stalla GK, Arzt E. Effect of SOM230 (pasireotide) on corticotroph cells: action in dogs with Cushing's disease. *Neuroendocrinology* 2011; 94: 124–136

Castinetti F, Saveanu A, Morange I, Brue T. Lanreotide for the treatment of acromegaly. *Adv Ther* 2009; 26: 600–612

Cattaneo MG, Amoroso D, Gussoni G, Sanguini AM, Vicentini LM. A somatostatin analogue inhibits MAP kinase activation and cell proliferation in human neuroblastoma and in human small cell lungcarcinoma cell lines. *FEB. Lett* 1996; 397: 164-168

Cattaneo MG, Scita G, Vicentini LM. Somatostatin inhibits PDGF-stimulated Ras activation in human neuroblastoma cells. *FEBS Lett* 1999; 459: 64-68

Chahal HS, Trivellin G, Leontiou CA, Alband N, Fowkes RC, Tahir A, Igreja SC, Chapple JP, Jordan S, Lupp A, Schulz S, Ansorge O, Karavitaki N, Carlsen E, Wass JA, Grossman AB, Korbonits M. Somatostatin analogs modulate AIP in somatotroph adenomas: the role of the ZAC1 pathway. *J Clin Endocrinol Metab* 2012; 97(8): E1411-20

Cho EY, Cho DI, Park JH, Kurose H, Caron MG, Kim KM. Roles of protein kinase C and actin-binding protein 280 in the regulation of intracellular trafficking of dopamine D3 receptor. *Mol Endocrinol* 2007; 21(9): 2242-54

Clemmons DR. The relative roles of growth hormone and IGF-1 in controlling insulin sensitivity. *J Clin Invest* 2004; 113(1): 25–27

Colao A, Pivonello R, Auriemma RS, De Martino MC, Bidlingmaier M, Briganti F, Tortora F, Burman P, Kourides IA, Strasburger CJ, Lombardi G. Efficacy of 12-month treatment with the GH receptor antagonist pegvisomant in patients with acromegaly resistant to long-term, high-dose somatostatin analog treatment: effect on IGF-I levels, tumor mass, hypertension and glucose tolerance. *Eur J Endocrinol* 2006; 154: 467–477

Corbetta S, Ballaré E, Mantovani G, Lania A, Losa M, Di Blasio AM, Spada A. Somatostatin receptor subtype 2 and 5 in human GH-secreting pituitary adenomas: analysis of gene sequence and mRNA expression. *Eur J Clin Invest* 2001; 31: 208–214

Cordelier P, Estève JP, Bousquet C, Delesque N, O'Carroll AM, Schally AV, Vaysse N, Susini C, Buscail L. Characterization of the antiproliferative signal mediated by the somatostatin receptor subtype sst5. *Proc Natl Acad Sci USA* 1997; 94(17): 9343-8

Córdoba-Chacón J, Gahete MD, Duran-Prado M, Pozo-Salas AI, Malagón MM, Gracia-Navarro F, Kineman RD, Luque RM, Castaño JP. Identification and characterization of new functional truncated variants of somatostatin receptor subtype 5 in rodents. *Cell Mol Life Sci* 2010; 67(7): 1147-63

Cozzi R, Attanasio R, Lodrini S, Lasio G. Cabergoline addition to depot somatostatin analogues in resistant acromegalic patients: efficacy and lack of predictive value of prolactin status. *Clin Endocrinol (Oxf)* 2004; 61: 209–215

Durán-Prado M, Gahete MD, Martínez-Fuentes AJ, Luque RM, Quintero A, Webb SM, Benito-López P, Leal A, Schulz S, Gracia-Navarro F, Malagón MM, Castaño JP. Identification and characterization of two novel truncated but functional isoforms of the somatostatin receptor subtype 5 differentially present in pituitary tumors. *J Clin Endocrinol Metab* 2009; 94(7): 2634-43

Durán-Prado M, Saveanu A, Luque RM, Gahete MD, Gracia-Navarro F, Jaquet P, Dufour H, Malagón MM, Culler MD, Barlier A, Castaño JP. A potential inhibitory role for the new truncated variant of somatostatin receptor 5, sst5TMD4, in pituitary adenomas poorly responsive to somatostatin analogs. *J Clin Endocrinol Metab* 2010; 95(5): 2497-502

Durán-Prado M, Gahete MD, Hergueta-Redondo M, Martínez-Fuentes AJ, Córdoba-Chacón J, Palacios J, Gracia-Navarro F, Moreno-Bueno G, Malagón MM, Luque RM, Castaño JP. The new truncated somatostatin receptor variant sst5TMD4 is associated to poor prognosis in breast cancer and increases malignancy in MCF-7 cells. *Oncogene* 2012; 31(16): 2049-61

Engqvist-Goldstein AE, Drubin DG. Actin assembly and endocytosis: from yeast to mammals. *Annu Rev Cell Dev Biol* 2003; 19: 287-332

Fahlbusch R, Keller B, Ganslandt O, Kreutzer J, Nimsky C. Transsphenoidal surgery in acromegaly investigated by intraoperative high-field magnetic resonance imaging. *Eur J Endocrinol* 2005; 153(2): 239-248

Ferjoux G, Lopez F, Esteve JP, Ferrand A, Vivier E, Vely F, Saint-Laurent N, Pradayrol L, Buscail L, Susini C. Critical role of Src and SHP-2 in sst2 somatostatin receptor-mediated activation of SHP-1 and inhibition of cell proliferation. *Mol Biol Cell* 2003; 14(9): 3911-28

Ferone D, de Herder WW, Pivonello R, Kros JM, van Koetsveld PM, de Jong T, Minuto F, Colao A, Lamberts SW, Hofland LJ. Correlation of in vitro and in vivo somatotropic adenoma responsiveness to somatostatin analogs and dopamine agonists with immunohistochemical evaluation of somatostatin and dopamine receptors and electron microscopy. *J Clin Endocrinol Metab* 2008; 93: 1412–1417

Ferrante E, Pellegrini C, Bondioni S, Peverelli E, Locatelli M, Gelmini P, Luciani P, Peri A, Mantovani G, Bosari S, Beck-Peccoz P, Spada A, Lania A. Octreotide promotes apoptosis in human somatotroph tumor cells by activating somatostatin receptor type 2. *Endocr Relat Cancer* 2006; 13(3): 955-62

Filopanti M, Ronchi C, Ballarè E, Bondioni S, Lania AG, Losa M, Gelmini S, Peri A, Orlando C, Beck-Peccoz P, Spada A. Analysis of somatostatin receptors 2 and 5 polymorphisms in patients with acromegaly. *J Clin Endocrinol Metab* 2005; 90: 4824–4828

Fleseriu M. The role of combination medical therapy in acromegaly: hope for the nonresponsive patient. *Curr Opin Endocrinol Diabetes Obes* 2013; 20(4): 321-9

Florio T, Arena S, Thellung S, Iuliano R, Corsaro A, Massa A, Pattarozzi A, Bajetto A, Trapasso F, Fusco A, Schettini G. The activation of the phosphotyrosine phosphatase η (r-PTP η) is responsible for the somatostatin inhibition of PC Cl3 thyroid cell proliferation. *Mol Endocrinol* 2001; 15: 1838–1852

Fougner SL, Bollerslev J, Latif F, Hald JK, Lund T, Ramm-Pettersen J, Berg JP. Low levels of raf kinase inhibitory protein in growth hormone-secreting pituitary adenomas correlate with poor response to octreotide treatment. *J Clin Endocrinol Metab* 2008; 93(4): 1211-6

Fox L, Alford M, Achim C, Mallory M, Masliah E. Neurodegeneration of somatostatin-immunoreactive neurons in HIV encephalitis. *J Neuropathol Exp Neurol* 1997; 56: 360-368

Frank G, Pasquini E, Farneti G, Mazzatenta D, Sciarretta V, Grasso V, Faustini FM. The endoscopic versus the traditional approach in pituitary surgery. *Neuroendocrinology* 2006; 83(3-4): 240-248

Frohman LA, Downs TR, Chomczynski P. Regulation of growth hormone secretion. *Front Neuroendocrinol* 1992; 13(4): 344-405

Gadelha MR, Kasuki L, Korbonits M. Novel pathway for somatostatin analogs in patients with acromegaly. *Trends Endocrinol Metab*2013; 24: 238–246

Gaidarov I, Santini F, Warren RA, Keen JH. Spatial control of coated-pit dynamics in living cells. *Nat Cell Biol* 1999; 1(1): 1-7

Gama R, Teale JD, Wright J, Ferns G, Marks V. Hyperproinsulinemia in acromegaly: evidence for abnormal pancreatic β-cell function. *Ann Clin Biochem* 1997; 34: 726-631

Gatto F, Feelders R, van der Pas R, Kros JM, Dogan F, van Koetsveld PM, van der Lelij AJ, Neggers SJ, Minuto F, de Herder W, Lamberts SW, Ferone D, Hofland LJ. β-Arrestin 1 and 2 and G protein-coupled receptor kinase 2 expression in pituitary adenomas: role in the regulation of response to somatostatin analogue treatment in patients with acromegaly. *Endocrinology* 2013; 154(12): 4715-25

Gatto F, Biermasz NR, Feelders RA, Kros JM, Dogan F, van der Lely AJ, Neggers SJ, Lamberts SW, Pereira AM, Ferone D, Hofland LJ. Low beta-arrestin expression correlates with the responsiveness to long-term somatostatin analog treatment in acromegaly. *Eur J Endocrinol* 2016; 174(5): 651-62

Ghosh M, Schonbrunn A. Differential temporal and spatial regulation of somatostatin receptor phosphorylation and dephosphorylation. *J Biol Chem* 2011; 286(15): 13561-73

Giustina A, Barkan A, Casanueva FF, Cavagnini F, Frohman L, Ho K, Veldhuis J, Wass J, Von Werder K, Melmed S. Criteria for cure of acromegaly: a consensus statement. *J Clin Endocrinol Metab* 2000; 85(2): 526-9

Giustina A, Casanueva FF, Cavagnini F, Chanson P, Clemmons D, Frohman LA, Gaillard R, Ho K, Jaquet P, Kleinberg DL, Lamberts SW, Lombardi G, Sheppard M, Strasburger CJ, Vance ML, Wass JA, Melmed S. Diagnosis and treatment of acromegaly complications. Pituitary Society and the European Neuroendocrine Association. *J Endocrinol Invest* 2003; 26(12): 1242-7

Gola M, Bonadonna S, Mazziotti G, Amato G, Giustina A. Resistance to somatostatin analogs in acromegaly: an evolving concept? *J Endocrinol Invest* 2006; 29: 86–93

Gomez-Pan A, Snow MH, Piercy DA, Robson V, Wilkinson R, Hall R, Evered DC. Actions of growth hormone inhibiting hormone (somatostatin) on the renin aldosterone system. *J Clin Endocrinol Metab* 1976; 43: 240-243

Grant M, Alturaihi H, Jaquet P, Collier B, Kumar U. Cell growth inhibition and functioning of human somatostatin receptor type 2 are modulated by receptor heterodimerization. *Mol Endocrinol* 2008; 22(10): 2278-92

Greenman Y, Tordjman K, Kisch E, Razon N, Ouaknine G, Stern NY. Relative sparing of anterior pituitary function in patients with growth hormone-secreting macroadenomas: comparison with nonfunctioning macroadenomas. *J Clin Endocrinol Metab* 1995; 80(5): 1577–1583

Grouselle D, Winsky-Sommerer R, David JP, Delacoutre A, Dournaud P, Epelbaum J. Loss of somatostatin-like immunoreactivity in the frontal cortex of Alzheimer patients carrying the apolipoprotein epsilon 4 allele. *Neurosci Lett* 1998; 255: 21-24

Grunstein RR, Ho KY, Sullivan CE. Sleep apnea in acromegaly. *Ann Intern Med* 1991; 115(7): 527-32

Guillermet J, Saint-Laurent N, Rochaix P, Cuvillier O, Levade T, Schally AV, Pradayrol L, Buscail L, Susini C, Bousquet C. Somatostatin receptor subtype 2 sensitizes human pancreatic cancer cells to death ligand-induced apoptosis. *Proc Natl Acad Sci USA* 2003; 100: 155–160

Guillermet-Guibert J, Saint-Laurent N, Davenne L, Rochaix P, Cuvillier O, Culler MD, Pradayrol L, Buscail L, Susini C, Bousquet C. Novel synergistic mechanism for sst2 somatostatin and TNFalpha receptors to induce apoptosis: crosstalk between NF-kappaB and JNK pathways. *Cell Death Differ* 2007; 14(2): 197-208

Gurevich VV, Gurevich EV. The structural basis of arrestin-mediated regulation of G-protein-coupled receptors. *Pharmacol Ther* 2006; 110(3): 465-502

Hall RA, Premont RT, Chow CW, Blitzer JT, Pitcher JA, Claing A, Stoffel RH, Barak LS, Shenolikar S, Weinman EJ, Grinstein S, Lefkowitz RJ. The beta2-adrenergic receptor interacts with the Na+/H+-exchanger regulatory factor to control Na+/H+ exchange. *Nature* 1998; 392(6676): 626-30

Hartwig JH, Stossel TP. Isolation and properties of actin, myosin, and a new actinbinding protein in rabbit alveolar macrophages. *J Biol Chem* 1975; 250(14): 5696-705

Hipkin RW, Friedman J, Clark RB, Eppler CM, Schonbrunn A. Agonist-induced desensitization, internalization, and phosphorylation of the sst2A somatostatin receptor. *J Biol Chem* 1997; 272(21): 13869-76

Hipkin RW, Wang Y, Schonbrunn A. Protein kinase C activation stimulates the phosphorylation and internalization of the sst2A somatostatin receptor. *J Biol Chem* 2000; 275(8): 5591-9

Holdaway IM, Rajasoorya C. Epidemiology of acromegaly. *Pituitary* 1999; 2: 29-41

Holdaway IM, Rajasoorya RC, Gamble GD. Factors influencing mortality in acromegaly. *J Clin Endocrinol Metab* 2004; 89: 667–674

Horvath A, Stratakis CA. Clinical and molecular genetics of acromegaly: MEN1, Carney complex, McCune-Albright syndrome, familial acromegaly and genetic defects in sporadic tumors. *Rev Endocr Metab Disord* 2008; 9(1): 1-11

Jaqaman K, Loerke D, Mettlen M, Kuwata H, Grinstein S, Schmid SL, Danuser G. Robust single-particle tracking in live-cell time-lapse sequences. *Nat Methods* 2008; 5(8): 695-702

Kaltsas GA, Mukherjee JJ, Jenkins PJ, Satta MA, Islam N, Monson JP, Besser GM, Grossman AB. Menstrual irregularity in women with acromegaly. *J Clin Endocrinol Metab* 1999; 84(8): 2731-5

Kao YJ, Ghosh M, Schonbrunn A. Ligand-dependent mechanisms of sst2A receptor trafficking: role of site-specific phosphorylation and receptor activation in the actions of biased somatostatin agonists. *Mol Endocrinol* 2011; 25(6): 1040-54

Kasai RS, Suzuki KG, Prossnitz ER, Koyama-Honda I, Nakada C, Fujiwara TK, Kusumi A. Full characterization of GPCR monomer-dimer dynamic equilibrium by single molecule imaging. *J Cell Biol* 2011; 192(3): 463-80

Katznelson L. Alterations in body composition in acromegaly. *Pituitary* 2009;12(2):136-42

Keppler A, Gendreizig S, Gronemeyer T, Pick H, Vogel H, Johnsson K. A general method for the covalent labeling of fusion proteins with small molecules in vivo. *Nat Biotechnol* 2003; 21(1): 86-9

Kim KM, Gainetdinov RR, Laporte SA, Caron MG, Barak LS. G protein-coupled receptor kinase regulates dopamine D3 receptor signaling by modulating the stability of a receptor-filamin-beta-arrestin complex. A case of autoreceptor regulation. *J Biol Chem* 2005; 280(13): 12774-80

Koenig JA, Edwardson JM, Humphrey PP. Somatostatin receptors in Neuro2A neuroblastoma cells: ligand internalization. *Br J Pharmacol* 1997; 120(1): 52-9

Koenig JA, Kaur R, Dodgeon I, Edwardson JM, Humphrey PP. Fates of endocytosed somatostatin sst2 receptors and associated agonists. *Biochem J* 1998; 336(Pt 2): 291-8

Kohout TA, Lefkowitz RJ. Regulation of G protein-coupled receptor kinases and arrestins during receptor desensitization. *Mol Pharmacol* 2003; 63: 9–18

Kusumi A, Sako Y, Yamamoto M. Confined lateral diffusion of membrane receptors as studied by single particle tracking (nanovid microscopy). Effects of calcium-induced differentiation in cultured epithelial cells. *Biophys J* 1993; 65(5): 2021-40

Lania A, Mantovani G, Spada A. Genetic abnormalities of somatostatin receptors in pituitary tumors. *Mol Cell Endocrinol* 2008; 286(1-2): 180-6

Lehmann A, Kliewer A, Schütz D, Nagel F, Stumm R, Schulz S. Carboxyl-terminal multi-site phosphorylation regulates internalization and desensitization of the human sst2 somatostatin receptor. *Mol Cell Endocrinol* 2014; 387(1-2): 44-51

Lelouvier B, Tamagno G, Kaindl AM, Roland A, Lelievre V, Le Verche V, Loudes C, Gressens P, Faivre-Baumann A, Lenkei Z, Dournaud P. Dynamics of somatostatin type 2A receptor cargoes in living hippocampal neurons. *J Neurosci* 2008; 28(17): 4336-49

Lesche S, Lehmann D, Nagel F, Schmid HA, Schulz S. Differential effects of octreotide and pasireotide on somatostatin receptor internalization and trafficking in vitro. *J Clin Endocrinol Metab* 2009; 94(2): 654-61

Lewis I, Bauer W, Albert R, Chandramouli N, Pless J, Weckbecker G, Bruns C. A novel somatostatin mimic with broad somatotropin release inhibitory factor receptor binding and superior therapeutic potential. *J Med Chem* 2003; 46: 2334–2344

Lin R, Karpa K, Kabbani N, Goldman-Rakic P, Levenson R. Dopamine D2 and D3 receptors are linked to the actin cytoskeleton via interaction with filamin A. *Proc Natl Acad Sci USA* 2001; 98(9): 5258-63

Lin R, Canfield V, Levenson R. Dominant negative mutants of filamin A block cell surface expression of the D2 dopamine receptor. *Pharmacology* 2002; 66(4): 173-81

Liu Q, Cescato R, Dewi DA, Rivier J, Reubi JC, Schonbrunn A. Receptor signaling and endocytosis are differentially regulated by somatostatin analogs. *Mol Pharmacol* 2005; 68(1): 90-101

Liu Q, Dewi DA, Liu W, Bee MS, Schonbrunn A. Distinct phosphorylation sites in the SST2A somatostatin receptor control internalization, desensitization, and arrestin binding. *Mol Pharmacol* 2008; 73(2): 292-304

Lopez F, Esteve JP, Buscali L, Delesqu N, Saint-Laurent N, Theveniau M, Nahmias C, Vaysse N, Susini C. The tyrosine phosphatase SHP-1 associates with the sst2 somatostatin receptor and is an essential component of sst2-mediated inhibitory growth signaling. *J Biol Chem* 1997; 272: 24448–24454

Ludvigsen E, Stridsberg M, Taylor JE, Culler MD, Oberg K, Janson ET, Sandler S. Regulation of insulin and glucagons secretion from rat pancreatic islet in vitro by somatostatin analogues. *Regul Pept* 2007; 10;138(1): 1-9

Luque RM, Rodríguez-Pacheco F, Tena-Sempere M, Gracia-Navarro F, Malagón MM, Castaño JP. Differential contribution of nitric oxide and cGMP to the stimulatory effects of growth hormone-releasing hormone and low-concentration somatostatin on growth hormone release from somatotrophs. *J Neuroendocrinol* 2005; 17(9): 577–582

Luque RM, Ibáñez-Costa A, Neto LV, Taboada GF, Hormaechea-Agulla D, Kasuki L, Venegas-Moreno E, Moreno-Carazo A, Gálvez MÁ, Soto-Moreno A, Kineman RD, Culler MD, Gahete MD, Gadelha MR, Castaño JP. Truncated somatostatin receptor variant sst5TMD4 confers aggressive features (proliferation, invasion and reduced octreotide response) to somatotropinomas. *Cancer Lett* 2015; 359(2): 299-306

Luttrell LM, Lefkowitz RJ. The role of beta-arrestins in the termination and transduction of G-protein-coupled receptor signals. *J Cell Sci* 2002; 115: 455–465

McKeage K, Cheer S, Wagstaff AJ. Octreotide long-acting release (LAR). A review of its use in the management of acromegaly. *Drugs* 2003; 63: 2473–2499

Melmed S, Braunstein GD, Horvath E, Ezrin C, Kovacs K. Pathophysiology of acromegaly. *Endocr Rev* 1983; 4(3): 271-90

Melmed S. Acromegaly and cancer: not a problem? *J Clin Endocrinol Metab* 2001; 86: 2929-34

Melmed S, Colao A, Barkan A, Molitch M, Grossman AB, Kleinberg D, Clemmons D, Chanson P, Laws E, Schlechte J, Vance ML, Ho K, Giustina A. Guidelines for acromegaly management: an update. *J Clin Endocrinol Metab* 2009; 94: 1509–1517

Merrifield CJ, Feldman ME, Wan L, Almers W. Imaging actin and dynamin recruitment during invagination of single clathrin-coated pits. *Nat Cell Biol* 2002; 4(9): 691-8

Meyerhof W. The elucidation of somatostatin receptor functions: a current view. Rev *Physiol Biochem Pharmacol* 1998; 133: 55–108

Minsaas L, Planagumà J, Madziva M, Krakstad BF, Masià-Balagué M, Katz AA, Aragay AM. Filamin a binds to CCR2B and regulates its internalization. *PLoS One* 2010; 5(8): e12212

Molitch ME. Clinical manifestations of acromegaly. *Endocrinol Metab Clin North Am* 1992; 21(3): 597-614

Moller LN, Stidsen CE, Hartmann B, Holst JJ. Somatostatin receptors. *Biochim Biophys Acta* 2003; 1616: 1-84

Muriel O, Echarri A, Hellriegel C, Pavón DM, Beccari L, Del Pozo MA. Phosphorylated filamin A regulates actin-linked caveolae dynamics. *J Cell Sci* 2011; 124(Pt 16): 2763-76

Nagel F, Doll C, Pöll F, Kliewer A, Schröder H, Schulz S. Structural determinants of agonist-selective signaling at the sst(2A) somatostatin receptor. *Mol Endocrinol* 2011; 25: 859–866

Najib S, Saint-Laurent N, Estève JP, Schulz S, Boutet-Robinet E, Fourmy D, Lättig J, Mollereau C, Pyronnet S, Susini C, Bousquet C. A switch of G protein-coupled receptor binding preference from phosphoinositide 3-kinase (PI3K)-p85 to filamin A negatively controls the PI3K pathway. Mol *Cell Biol* 2012; 32(5): 1004-16

Nakamura F, Stossel TP, Hartwig JH. The filamins: organizers of cell structure and function. *Cell Adh Migr* 2011; 5(2): 160-9

Nielsen S, Mellemkjaer S, Rasmussen LM, Ledet T, Olsen N, Bojsen-Møller M, Astrup J, Weeke J, Jørgensen JO. Expression of somatostatin receptors on human pituitary adenomas in vivo and ex vivo. *J Endocrinol Invest* 2001; 24: 430–437

Nikolaev VO, Bünemann M, Hein L, Hannawacker A, Lohse MJ. Novel single chain cAMP sensors for receptor-induced signal propagation. *J Biol Chem* 2004; 279(36): 37215-8

Noam Y, Ehrengruber MU, Koh A, Feyen P, Manders EM, Abbott GW, Wadman WJ, Baram TZ. Filamin A promotes dynamin-dependent internalization of hyperpolarization-activated cyclic nucleotide-gated type 1 (HCN1) channels and restricts Ih in hippocampal neurons. *J Biol Chem* 2014; 289(9): 5889-903

Oakley RH, Laporte SA, Holt JA, Caron MG, Barak LS. Differential affinities of visual arrestin, beta arrestin1, and beta arrestin2 for G protein-coupled receptors delineate two major classes of receptors. *J Biol Chem* 2000; 275(22): 17201-10

Oakley RH, Laporte SA, Holt JA, Barak LS, Caron MG. Molecular determinants underlying the formation of stable intracellular G protein-coupled receptor-beta-arrestin complexes after receptor endocytosis. *J Biol Chem* 2001; 276(22): 19452-60

Olias G, Viollet C, Kusserow H, Epelbaum J, Meyerhof W. Regulation and function of somatostatin receptors. *J Neurochem* 2004; 89: 1057–1091

Onoprishvili I, Andria ML, Kramer HK, Ancevska-Taneva N, Hiller JM, Simon EJ. Interaction between the mu opioid receptor and filamin A is involved in receptor regulation and trafficking. *Mol Pharmacol* 2003; 64(5): 1092-100

Oriola J, Lucas T, Halperin I, Mora M, Perales MJ, Alvarez-Escolá C, Paz de MN, Díaz Soto G, Salinas I, Julián MT, Olaizola I, Bernabeu I, Marazuela M, Puig-Domingo M. Germline mutations of AIP gene in somatotropinomas resistant to somatostatin analogues. *Eur J Endocrinol* 2012; 168(1): 9-13

Pagès P, Benali N, Saint-Laurent N, Estève JP, Schally AV, Tkaczuk J, Vaysse N, Susini C, Buscail L. sst2 somatostatin receptor mediates cell cycle arrest and induction of p27(Kip1). Evidence for the role of SHP-1. *J Biol Chem* 1999; 274(21): 15186-93

Pan MG, Florio T, Stork PJ. G protein activation of a hormone-stimulated phosphatase in human tumor cells. *Science* 1992; 256: 1215–1217

Patel YC, Greenwood MT, Warszynska A, Panetta R & Srikant CB. All five cloned human somatostatin receptors (hSSTR1-5) are functionally coupled to adenylyl cyclase. *Biochem Biophys Res Commun* 1994; 198: 605–612

Patel YC, Greenwood MT, Panetta R, Demchyshyn L, Niznik H, Srikant CB. The somatostatin receptor family. *Life Sci* 1995;57(13):1249-65

Patel YC. Somatostatin and its receptor family. *Front Neuroendocrinol* 1999; 20: 157–198

Pernicone PJ, Scheithauer BW, Sebo TJ, Kovacs KT, Horvath E, Young WF, Lloyd RV, Davis DH, Guthrie BL, Schoene WC. Pituitary carcinoma: a clinicopathologic study of 15 cases. *Cancer* 1997; 79: 804-12

Petersenn S, Heyens M, Lüdecke DK, Beil FU, Schulte HM. Absence of somatostatin receptor type 2A mutations and gip oncogene in pituitary somatotroph adenomas. *Clin Endocrinol (Oxf)* 2000; 52: 35–42

Peverelli E, Mantovani G, Calebiro D, Doni A, Bondioni S, Lania A, Beck-Peccoz P, Spada A. The third intracellular loop of the human somatostatin receptor 5 is crucial for arrestin binding and receptor internalization after somatostatin stimulation. *Mol Endocrinol* 2008; 22(3): 676-88

Peverelli E, Lania AG, Mantovani G, Beck-Peccoz P, Spada A. Characterization of intracellular signaling mediated by human somatostatin receptor 5: role of the DRY motif and the third intracellular loop. *Endocrinology* 2009; 150(7): 3169-76

Peverelli E, Mantovani G, Vitali E, Elli FM, Olgiati L, Ferrero S, Laws ER, Della Mina P, Villa A, Beck-Peccoz P, Spada A, Lania AG. Filamin-A is essential for dopamine d2 receptor expression and signaling in tumorous lactotrophs. *J Clin Endocrinol Metab* 2012; 97(3): 967-77

Peverelli E, Busnelli M, Vitali E, Giardino E, Galés C, Lania AG, Beck-Peccoz P, Chini B, Mantovani G, Spada A. Specific roles of G(i) protein family members revealed by dissecting SST5 coupling in human pituitary cells. *J Cell Sci* 2013; 126(Pt 2): 638-44

Peverelli E, Giardino E, Treppiedi D, Vitali E, Cambiaghi V, Locatelli M, Lasio GB, Spada A, Lania AG, Mantovani G. Filamin A (FLNA) plays an essential role in somatostatin receptor 2 (SST2) signaling and stabilization after agonist stimulation in human and rat somatotroph tumor cells. *Endocrinology* 2014; 155(8): 2932-41

Planagumà J, Minsaas L, Pons M, Myhren L, Garrido G, Aragay AM. Filamin A-hinge region 1-EGFP: a novel tool for tracking the cellular functions of filamin A in real-time. *PLoS One* 2012; 7(8): e40864

Plöckinger U, Albrecht S, Mawrin C, Saeger W, Buchfelder M, Petersenn S, Schulz S. Selective loss of somatostatin receptor 2 in octreotide-resistant growth hormone-secreting adenomas. *J Clin Endocrinol Metab* 2008; 93: 1203–1210

Pöll F, Lehmann D, Illing S, Ginj M, Jacobs S, Lupp A, Stumm R, Schulz S. Pasireotide and octreotide stimulate distinct patterns of sst2A somatostatin receptor phosphorylation. *Mol Endocrinol* 2010; 24(2): 436-46

Qualmann B, Kessels MM, Kelly RB. Molecular links between endocytosis and the actin cytoskeleton. *J Cell Biol* 2000; 150(5): F111-6

Qualmann B, Kessels MM. Endocytosis and the cytoskeleton. *Int Rev Cytol* 2002; 220: 93-144

Rappoport JZ, Kemal S, Benmerah A, Simon SM. Dynamics of clathrin and adaptor proteins during endocytosis. *Am J Physiol Cell Physiol* 2006; 291(5): C1072-81

Reid IA, Rose JC. An intrarenal effect of somatostatin on water excretion. *Endocrinology* 1977; 100: 782-785

Reisine T, Bell GI. Molecular biology of somatostatin receptors. *Endocr Rev* 1995; 16: 427–442

Renehan AG, O'Connell J, O'Halloran D, Shanahan F, Potten CS, O'Dwyer ST, Shalet SM. Acromegaly and colorectal cancer: a comprehensive review of epidemiology, biological mechanisms, and clinical implications. *Horm Metab Res* 2003; 35: 712-25

Rens-Domiano S, Reisine T. Biochemical and functional properties of somatostatin receptors. *J Neurochem* 1992; 58: 1987-1996

Resmini E, Dadati P, Ravetti JL, Zona G, Spaziante R, Saveanu A, Jaquet P, Culler MD, Bianchi F, Rebora A, Minuto F, Ferone D. Rapid pituitary tumor shrinkage with dissociation between antiproliferative and antisecretory effects of a long-acting octreotide in an acromegalic patient. *J Clin Endocrinol Metab* 2007; 92: 1592–1599

Reubi JC, Heitz PU, Landolt AM. Visualization of somatostatin receptors and correlation with immunoreactive growth hormone and prolactin in human pituitary adenomas: evidence for different tumor subclasses. *J Clin Endocrinol Metab* 1987; 65(1): 65-73

Reubi JC, Landolt AM. The growth hormone responses to octreotide in acromegaly correlate with adenoma somatostatin receptor status. *J Clin Endocrinol Metab* 1989; 68: 844–850

Reubi JC, Waser B, Schaer JC, Laissue JA. Somatostatin receptor sst1-sst5 expression in normal and neoplastic human tissues using receptor autoradiography with subtype-selective ligands. *Eur J Nucl Med* 2001; 28: 836-846

Richardson UI, Schonbrunn A. Inhibition of adrenocorticotropin secretion by somatostatin in pituitary cells in culture. *Endocrinology* 1981; 108(1): 281-90

Robertson SP, Twigg SR, Sutherland-Smith AJ, Biancalana V, Gorlin RJ, Horn D, Kenwrick SJ, Kim CA, Morava E, Newbury-Ecob R, Orstavik KH, Quarrell OW, Schwartz CE, Shears DJ, Suri M, Kendrick-Jones J, Wilkie AO; OPD-spectrum Disorders Clinical Collaborative Group. Localized mutations in the gene encoding the cytoskeletal protein filamin A cause diverse malformations in humans. *Nat Genet* 2003; 33(4): 487-91

Rocheville M, Lange DC, Kumar U, Sasi R, Patel RC, Patel YC. Subtypes of somatostatin receptor assemble as functional homo- and heterodimers. *J Biol Chem* 2000; 275: 7862–7869

Sandret L, Maison P, Chanson P. Place of cabergoline in acromegaly: a meta-analysis. *J Clin Endocrinol Metab* 2012; 96(5): 1327-35

Scott MG, Pierotti V, Storez H, Lindberg E, Thuret A, Muntaner O, Labbé-Jullié C, Pitcher JA, Marullo S. Cooperative regulation of extracellular signal-regulated kinase activation and cell shape change by filamin A and beta-arrestins. *Mol Cell Biol* 2006; 26(9): 3432-45

Seck T, Baron R, Horne WC. Binding of filamin to the C-terminal tail of the calcitonin receptor controls recycling. *J Biol Chem* 2003; 278(12): 10408-16

Sellers LA, Alderton F, Carruthers AM, Schindler M, Humphrey PP. Receptor isoforms mediate opposing proliferative effects through betagamma-activated p38 or Akt pathways. *Mol Cell Biol* 2000; 20: 5974–5985

Sharma K, Patel YC, Srikant CB. Subtype-selective induction of wild-type p53 and apoptosis, but not cell cycle arrest, by human somatostatin receptor 3. *Mol Endocrinol* 1996; 10: 1688–1696

Sheaves R, Jenkins P, Blackburn P, Huneidi AH, Afshar F, Medbak S, Grossman AB, Besser GM, Wass JA. Outcome of transsphenoidal surgery for acromegaly using strict criteria for surgical cure. *Clin Endocrinol (Oxf)* 1996; 45(4): 407-413

Shen LP, Pictet RL, Rutter WJ. Human somatostatin I: sequence of the cDNA. *Proc Natl Acad Sci USA* 1982; 79(15): 4575-9

Sheratori K, Watanabe S, Takeuchi T. Somatostatin analog, SMS 201-995, inhibits pancreatic exocrine secretion and release of secretin and cholecystokinin in rats. *Pancreas* 1991; 6: 23-30

Siler TM, Yen SC, Vale W, Guillemin R. Inhibition by somatostatin on the release of TSH induced in man by thyrotropin-releasing factor. *J Clin Endocrinol Metab* 1974; 38: 742–745

Socin HV, Chanson P, Delemer B, Tabarin A, Rohmer V, Mockel J, Stevenaert A, Beckers A. The changing spectrum of TSH-secreting pituitary adenomas: diagnosis and management in 43 patients. *Eur J Endocrinol* 2003; 148: 433-42

Spada A, Arosio M, Bochicchio D, Bazzoni N, Vallar L, Bassetti M, Faglia G. Clinical, biochemical, and morphological correlates in patients bearing growth hormone-secreting pituitary tumors with or without constitutively active adenylyl cyclase. *J Clin Endocrinol Metab* 1990; 71(6): 1421-6

Stark A, Mentlein R. Somatostatin inhibits glucagon-like peptide-1-induced insulin secretion and proliferation of RINm5F insulinoma cells. *Regul Pept* 2002; 108: 97-102

Stavrou S, Kleinberg DL. Rheumatic manifestations of pituitary tumors. *Curr Rheumatol Rep* 2001; 3: 459-63

Stossel TP, Condeelis J, Cooley L, Hartwig JH, Noegel A, Schleicher M, Shapiro SS. Filamins as integrators of cell mechanics and signalling. *Nat Rev Mol Cell Biol* 2001; 2(2): 138-45

Strittmatter M, Hamann GF, Strubel D, Cramer H, Schimrigk K. Somatostatin-like immunoreactivity, its molecular forms and monoaminergic metabolites in aged and demented patiens with Parkinson's disease-effect of L-Dopa. *J Neural Transm Gen Sect* 1996; 103: 591-602

Strowbridge BW, Bean AJ, Spencer DD, Rpth RH, Shepherd GM, Robbins RJ. Low levels of somatostatin-like immunoreactivity in neocortex resected from presumed seizure foci in epileptic patients. *Brain Res* 1992; 587: 164-168

Sungkaworn T, Rieken F, Lohse MJ, Calebiro D. High-resolution spatiotemporal analysis of receptor dynamics by single-molecule fluorescence microscopy. *J Vis Exp* 2014; (89): e51784

Sverdlov M, Shinin V, Place AT, Castellon M, Minshall RD. Filamin A regulates caveolae internalization and trafficking in endothelial cells. *Mol Biol Cell* 2009; 20(21): 4531-40

Taboada GF, Luque RM, Bastos W, Guimarães RF, Marcondes JB, Chimelli LM, Fontes R, Mata PJ, Filho PN, Carvalho DP, Kineman RD, Gadelha MR. Quantitative analysis of somatostatin

receptor subtype (SSTR1-5) gene expression levels in somatotropinomas and non-functioning pituitary adenomas. *Eur J Endocrinol* 2007;156(1): 65-74

Taboada GF, Luque RM, Neto LV, Machado Ede O, Sbaffi BC, Domingues RC, Marcondes JB, Chimelli LM, Fontes R, Niemeyer P, de Carvalho DP, Kineman RD, Gadelha MR. Quantitative analysis of somatostatin receptor subtypes (1-5) gene expression levels in somatotropinomas and correlation to in vivo hormonal and tumor volume responses to treatment with octreotide LAR. *Eur J Endocrinol* 2008; 158: 295–303

Teijeiro R, Rios R, Costoya JA, Castro R, Bello JL, Devesa J, Arce VM. Activation of human somatostatin receptor 2 promotes apoptosis through a mechanism that is independent from induction of p53. *Cell Physiol Biochem* 2002; 12: 31–38 44

Thelin WR, Chen Y, Gentzsch M, Kreda SM, Sallee JL, Scarlett CO, Borchers CH, Jacobson K, Stutts MJ, Milgram SL. Direct interaction with filamins modulates the stability and plasma membrane expression of CFTR. *J Clin Invest* 2007; 117(2): 364-74

Thorner MO, Frohman LA, Leong DA., Thominet J, Downs T, Hellmann P, Chitwood J, Vaughan JM, Vale W. Extrahypothalamic growth-hormone-releasing factor (GRF) secretion is a rare cause of acromegaly: plasma GRF levels in 177 acromegalic patients. *J Clin Endocrinol Metab* 1984; 59(5): 846-849

Trainer PJ, Drake WM, Katznelson L, Freda PU, Herman-Bonert V, Van der LA, Dimaraki EV, Stewart PM, Friend KE, Vance ML, Besser GM, Scarlett JA, Thorner MO, Parkinson C, Klibanski A, Powell JS, Barkan AL, Sheppard MC, Malsonado M, Rose DR, Clemmons DR, Johannsson G, Bengtsson BA, Stavrou S, Kleinberg DL, Cook DM, Phillips LS, Bidlingmaier M, Strasburger CJ, Hackett S, Zib K, Bennett WF, Davis RJ. Treatment of acromegaly with the growth hormone-receptor antagonist pegvisomant. *N Engl J Med* 2000; 342(16): 1171-1177

Treppiedi D, Peverelli E, Giardino E, Ferrante E, Calebiro D, Spada A, Mantovani G. Somatostatin Receptor Type 2 (SSTR2) Internalization and Intracellular Trafficking in Pituitary GH-Secreting Adenomas: Role of Scaffold Proteins and Implications for Pharmacological Resistance. *Horm Metab Res* 2016; Epub ahead of print

Tsuji A, Kawasaki K, Ohnishi S, Merkle H, Kusumi A. Regulation of band 3 mobilities in erythrocyte ghost membranes by protein association and cytoskeletal meshwork. *Biochemistry* 1988; 27(19): 7447-52

Tulipano G, Bonfanti C, Milani G, Billeci B, Bollati A, Cozzi R, Maira G, Murphy WA, Poiesi C, Turazzi S, Giustina A. Differential inhibition of growth hormone secretion by analogs selective for somatostatin receptor subtypes 2 and 5 in human growth-hormone-secreting adenoma cells in vitro. *Neuroendocrinology* 2001; 73: 344–351

Tulipano G, Stumm R, Pfeiffer M, Kreienkamp HJ, Höllt V, Schulz S. Differential beta-arrestin trafficking and endosomal sorting of somatostatin receptor subtypes. *J Biol Chem* 2004; 279(20): 21374-82

Tuominen I, Heliövaara E, Raitila A, Rautiainen MR, Mehine M, Katainen R, Donner I, Aittomäki V, Lehtonen HJ, Ahlsten M, Kivipelto L, Schalin-Jäntti C, Arola J, Hautaniemi S, Karhu A. AIP inactivation leads to pituitary tumorigenesis through defective Gαi-cAMP signaling. *Oncogene* 2015; 34(9): 1174-84

Vale W, Rivier C, Brazeau P, Guillemin R. Effects of somatostatin on the secretion by thyrotropin and prolactin. *Endocrinology* 1974; 95: 968–977

van der Flier A, Sonnenberg A. Structural and functional aspects of filamins. *Biochim Biophys Acta* 2001; 1538(2-3): 99-117

van Hagen PM, Krenning EP, Kwekkeboom DJ, Reubi JC, Anker-Lugtenburg PJ, Löwenberg B, Lamberts SW. Somatosatin and the immune and hematopoetic system; a review. *Eur J Clin Invest* 1994; 24: 91–99

Neto VL, Machado E de O, Luque RM, Taboada GF, Marcondes JB, Chimelli LM, Quintella LP, Niemeyer P Jr, de Carvalho DP, Kineman RD, Gadelha MR. Expression analysis of dopamine receptor subtypes in normal human pituitaries, nonfunctioning pituitaryadenomas and somatotropinomas, and the association between dopamine and somatostatin receptors with clinical response to octreotide-LAR in acromegaly. *J Clin Endocrinol Metab* 2009; 94 1931–1937

Vitali E, Cambiaghi V, Zerbi A, Carnaghi C, Colombo P, Peverelli E, Spada A, Mantovani G, Lania AG. Filamin-A is required to mediate SST2 effects in pancreatic neuroendocrine tumours. *Endocr Relat Cancer* 2016; 23(3): 181-90

Wass JA, Thorner MO, Morris DV, Rees LH, Mason AS, Jones AE, Besser GM. Long-term treatment of acromegaly with bromocriptine. *Br Med J* 1977; 1(6065): 875-878

Zhang M, Breitwieser GE. High affinity interaction with filamin A protects against calcium-sensing receptor degradation. *J Biol Chem* 2005; 280(12): 11140-6